Utilization of Offshore Geothermal Resources for Power Production

by

Baldur Kárason

Thesis
Master of Science in Sustainable Energy Engineering

January 2013

Utilization of Offshore Geothermal Resources for Power Production

Baldur Kárason

Thesis submitted to the School of Science and Engineering at Reykjavík University in partial fulfillment of the requirements for the degree of

Master of Science in Sustainable Energy Engineering

January 2013

Thesis Committee

María S Guðjónsdóttir, Reykjavík University, Iceland – Supervisor
Dr. Páll Valdimarsson, Reykjavík University, Iceland – Supervisor

Examiner:

Kristinn Ingason
Mannvit hf.

Abstract

Today geothermal energy has been utilized on land worldwide and the geothermal resources have a potential of being one of the greatest sustainable energy choices there is. Offshore geothermal energy has not been considered a feasible option, but with increasing energy prices and increasing knowledge of the utilization of this resource the choice becomes more attractive. The main objective for the project described in this thesis was to analyze and compare a number of configurations for potential power production from offshore geothermal resources. The options were analyzed mainly with technical feasibility in mind. A rough estimation of the economic aspects was performed as well. The energy output was calculated and compared for different energy processes using data from the geothermal field in Reykjanes Iceland. The goal of this work was to establish a map of available options and opportunities within the offshore geothermal industry with Reykjanes ridge particularly in mind. The main results indicate that technically it is possible to construct offshore power plants, but the main disadvantage is the high cost compared to a traditional power plants located on land. The most feasible option is a power plant located on land connected to a wellhead on the ocean bed. Thermoelectricity could be a favorable future power option but at this point the specific electricity production per size of the device is too small.

Útdráttur

Jarðvarmi hefur til dagsins í dag verið beislaður á landi um allan heim og hefur alla burði til að verða stærsti einstaki sjálfbæri orkugjafinn. Nýting jarðvarma á hafi hefur hingað til ekki verið talin fýsilegur kostur en með hækkandi orkuverði sem og vaxandi þekkingu á almennri jarðvarmanýtingu gæti þessi kostur reynst fýsilegri. Helsta markið þessa verkefnis var að greina og bera saman nokkra orkuferla sem allir hafa það sameiginlegt að nýta vökva úr jarðvarmaholu sem staðsett er á hafsbotninum utan Reykjanes. Ferlarnir voru aðalega greindir með tæknilega hagkvæmni í huga. Einnig var gerð gróf greining á fjárhagslegri hagkvæmni ferlanna. Markmiðið með þessu verkefni er að greina þá möguleika sem í boði eru fyrir nýtingu jarðvarma á hafi með Reykjaneshrygginn sérstaklega í huga. Megin niðurstöður verkefnisins eru að tæknilega er ekkert því til fyrirstöðu að byggja og hanna jarðvarmavirkjun á hafi en stærsti ókosturinn er sá hve kostnaðarsöm slíkar virkjanir gætu verið miðað við hefðbundna jarðvarmavirkjun á landi. Hagkvæmasti valkosturinn er jarðvarmavirkjun staðsett á landi og tengd með rörum við holutoppslokan sem staðsettur er á hafsbotninum. Varmarafmagn gæti einnig verið vænn framtíðarkostur en á þessum tímapunkti er raforkuframleiðslan of lítil miðað við stærð búnaðarins sem til þarf.

Utilization of Offshore Geothermal Resources for Power Production

Baldur Kárason

Thesis submitted to the School of Science and Engineering
at Reykjavík University in partial fulfillment
of the requirements for the degree of
Master of Science in Sustainable Energy Engineering

January 2013

Student:

_____

Baldur Kárason

Supervisor:

_____

María S Guðjónsdóttir

Acknowledgements

I would like take the opportunity to thank my supervisor María S Guðjónsdóttir for her endless support and excellent guidance in all aspects of the project. I would also like to thank my assistant supervisor professor Dr. Páll Valdimarsson, who has provided excellent guidance throughout this project.

I also want to thank Sverrir þórhallsson and Páll Jónsson from Iceland Geosurvey, Geir Þórólfsson from HS-Orka and Árni Geirson from ALTA for their hands on experience and providing the necessary data needed for this project.

At last I give thanks to my wife Karen Jónsdóttir for her endless support and understanding, and to all the people that stood by me throughout this time.

Table of Contents

List of Tables

List of figures

Nomenclature

A	Area [m^2]
D	Diameter [m]
η	Efficiency [-]
h	Enthalpy [kJ/kg]
s	Entropy [kJ/kg K]
$\dot{Q}$	Heat transfer [J/s]
H	Height [m]
ṁ	Mass flow [kg/s]
P	Pressure [bar]
x	Steam quality [-]
T	Temperature [°C]
μ	Viscosity [Pa*s]
$\dot{W}$	Work [W]
σ	Standard deviation [-]
g	Gravitational acceleration [m/s^2]
v	Specific volume [m^3/kg]
$\dot{E}$	Exergy [kW]
$\dot{V}$	Volumetric flow rate [m^3/s]
t_m	Steel thickness [m]
f	Friction factor [-]
Re	Reynolds number [-]
ρ	Density [kg/m^3]
R	Thermal resistance [W/m^2 °C]

1. Introduction

The main focus of this project is offshore geothermal power plants utilizing offshore geothermal resources. The energy market in Iceland still has some potential to utilize energy on land, which is probably a less expensive option than an offshore power plant when it comes to investment cost and operation and maintenance cost per unit of energy produced. But if it was not for the concept of "*thinking outside the box*" Iceland would not be as advanced in geothermal technology as it is today. Being one step ahead when it comes to the latest technology would provide the Icelandic engineering companies a leading position in the offshore geothermal technology field. Utilization of offshore geothermal energy is not far away, the technology is already there. The project motivation is to extend the scope of geothermal energy utilization options by mapping available possibilities within the offshore geothermal industry.

The advantages of offshore power plants as opposed to land utilization are several, e.g. no need for a detailed visual environmental assessment although it will need some general environmental assessment. No land space is required or an extension of the actual energy fields, which is a big factor as available energy fields are decreasing every year. On the other hand the disadvantages are the economical sides of it, the same goes for almost all sustainable systems available on the market today.

The objective of this project is to analyze and compare a number of configurations for potential power production from offshore geothermal resources. These analyses are compared mainly with technical feasibility in mind. A rough estimation of the economic aspects is performed as well. The position of the power plant is given a particular emphasis and there are several options available.

The options are analyzed below and shown in Figure 24, Figure 27, Figure 28 and Figure 29.

- Platform based power plant where the steam goes through a pipeline from the seabed to the platform (Option A)
- Land based power plant separating the two phase fluid at the seabed then directing the pure steam onto land via pipeline (Option B)
- Underwater power plant producing electricity and transporting it to land (Option C)

- Binary power plant on land which uses a heat exchanger located at the seabed heating circulating working fluid. (Option D)
- A pipeline connected to a thermoelectric device using the temperature difference between the geothermal fluid and the ocean.

The location of the potential offshore power plants that was studied within this project is the Reykjanes ridge. There is already a 2x50 MW_e power plant operating on the peninsula of Reykjanes, Reykjanesvirkjun, and studies indicate that there is energy capacity to produce 50 MW_e or more [1]. The depth to the seabed along the ridge varies between 150-350 meters [2] and considered to be, at certain depths, shallow enough for controllable hydrostatic pressures for pipeline gathering system and underwater power plant. Figure 1 shows the actual depth to the seabed.

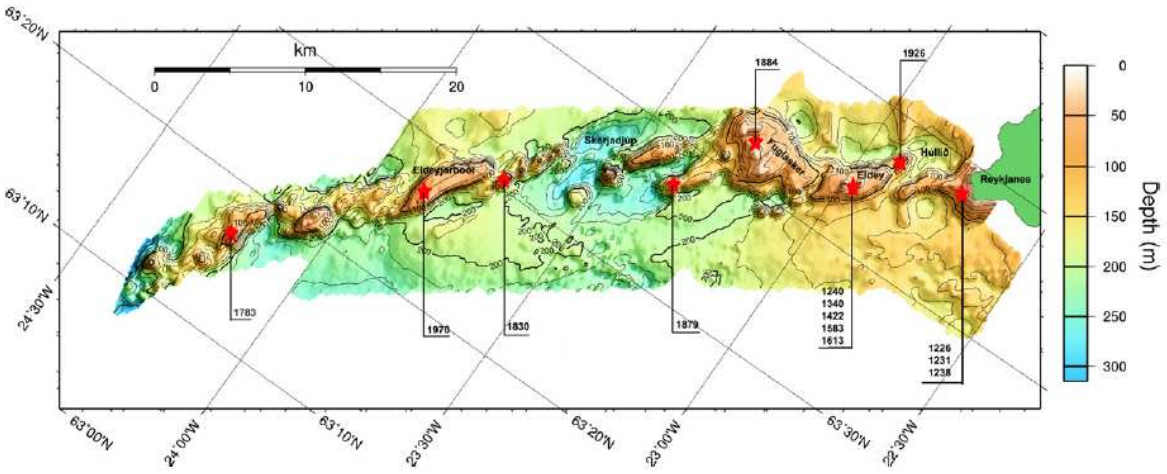

Figure 1 A map of Reykjanes ridge showing the actual depth to the seabed [2]

2. Literature Review

2.1. Worldwide Conditions for Offshore Projects

Much has not been done when it comes to the utilization of offshore geothermal energy. The main reason for this is that more economic options are on land than offshore. The development phase for offshore geothermal energy still has to go on so that future generations can benefit from earlier research phases. The research phases could e.g. be material chose for the pipe as well as what insulation would fit pipes located underwater best and assessment for weather conditions for areas where offshore projects might be constructed. In this section two projects that have high potentials to become the next offshore geothermal projects are summarized. Those two projects are the only projects under development that could be found in literature research.

2.1.1. Italia Marsili Project

The Italian institution Unione Geotermica Italiana has started research for potential areas for offshore geothermal. The research and development department in Italy is financing this project in hope of increasing the overall geothermal power output in Italy. The goal is to have an electricity production of 600 MW_e after 10 years and approximately 1200 MW_e after 15 years in the Marsili project [3]. The area that will be explored the most is the volcano mountain at the Tyrrhenian Sea. This area is estimated to have a potential of 1 GW_e [4]. The technology of the power utilization has not yet been published, and is probably still under research. The underwater volcano is shown on Figure 2.

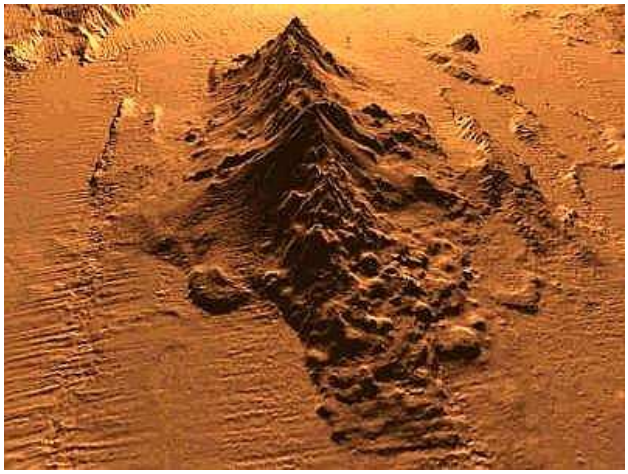

Figure 2 The underwater volcano Marsili (scale unknown) [4]

2.1.2. Hydrothermal Vents in the Gulf of California

The National University of Mexico has been developing a small submarine that could be located beside hydrothermal vents. Hydrothermal vents occur when a geothermal fluid flows from the ocean crust at saturation conditions. The fluid is so high enthalpic that it could be utilized for electricity production. The design for the submarine power plant is a binary cycle power plant with a turbine generator and a feed pump installed inside the submarine. From both ends of the submarine there are tubes formed in a spiral, one is to evaporate the working fluid with the heat from the hydrothermal vent and is located over the hydrothermal vent and the other spiral is for cooling down the working fluid with the cold sea. It uses the cold ocean to cool down the fluid within the spiral. When the working fluid is fully condensed it is pumped back into the spiral that lies over the hydrothermal vent. An artist's impression of the submarine is shown on Figure 3.

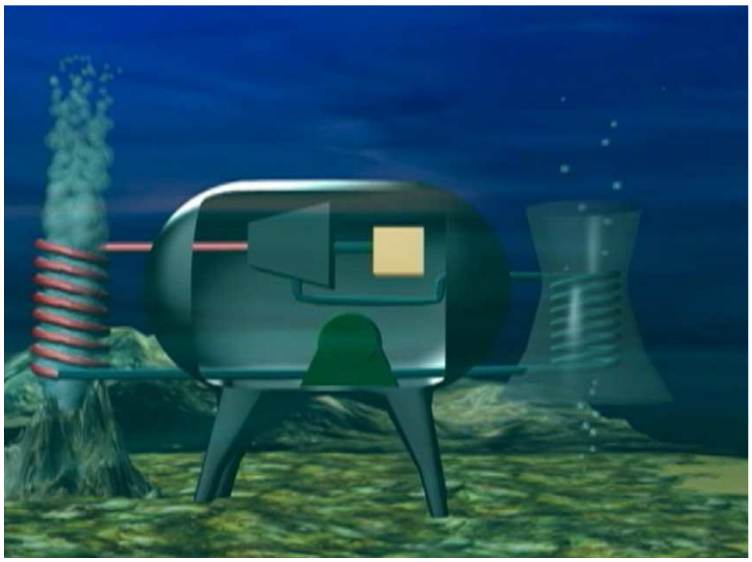

Figure 3 The submarine power plant utilizing hydrothermal vent [5]

It is estimated that only 1% of the existing hydrothermal vents have already been discovered [5]. If only 1% of the discovered hydrothermal vents could be exploited then estimations indicate that 130.000 MW_e could be generated. Research shows that from one hydrothermal vent with saturated water at temperature 365°C at depth 2000 meters to the ocean floor, and the hydrothermal vent with a diameter of 0,6 meter, around 20 MW_e could be generated [5]. This project is under development and is being tested in shallow seas near Mexico.

2.2. Possible Locations

Possible locations for offshore geothermal utilization around Iceland are marked with colored dots on Figure 4. The red dot north of Iceland is the island Grímsey and hydrothermal vents are to be found there [6]. The depth to the hydrothermal vents is approximately 400 meters but the biggest disadvantage for utilizing that offshore steam field is the location, far out in the sea, and the fact that Grímsey is not connected to the electrical grid of Iceland. On the other hand it could be good for the people living on the island Grímsey to utilize that source as they are producing electricity with diesel driven generators and heating their houses using oil.

In the southwest corner of Iceland you can see green and blue dots, the green dots indicate evidence of gas bubble and the blue dots indicate measured seismic activities. The location of Reykjanes is close to land, connected to the national grid and has some information available to estimate the behavior of the geothermal field.

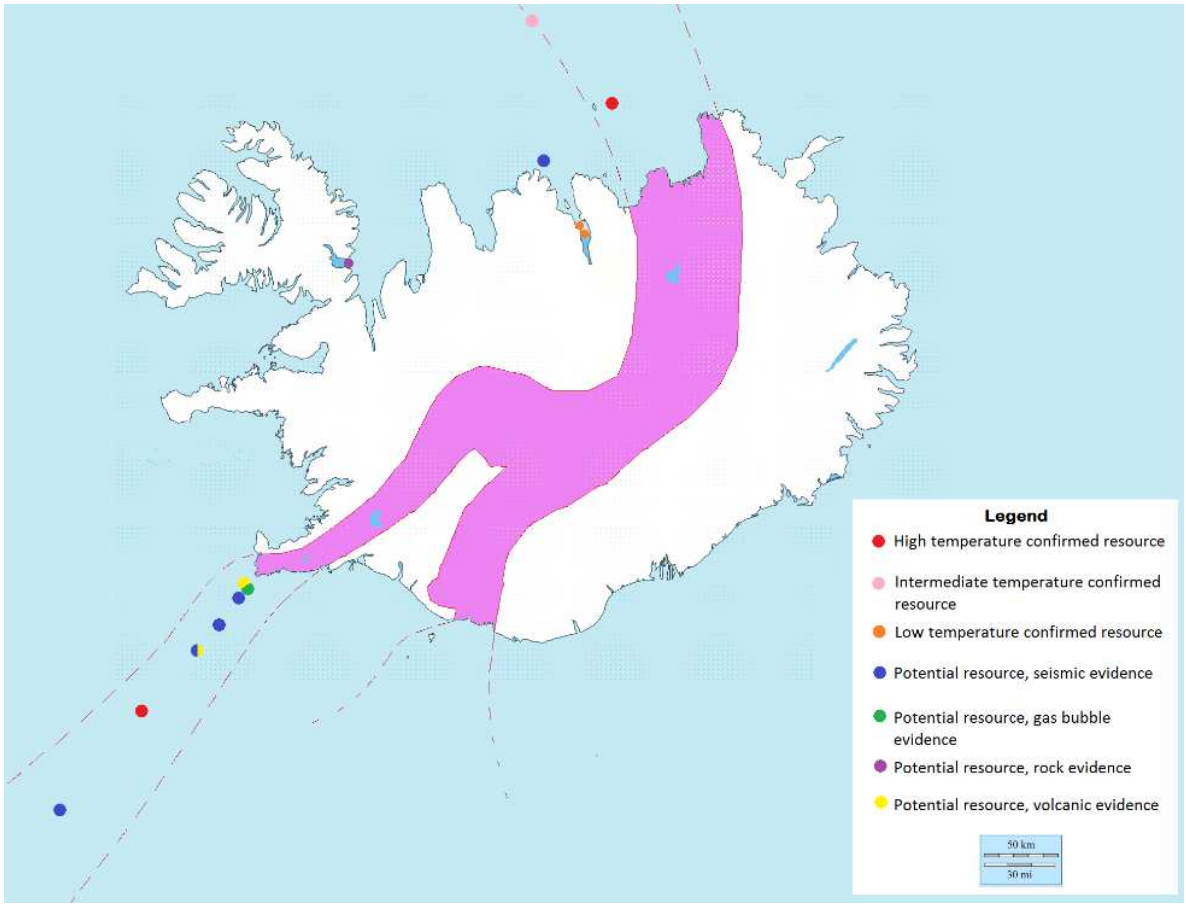

Figure 4 Map of Iceland showing known offshore hydrothermal vents [6]

2.2.1. Reykjanes Ridge

Figure 5 shows the Reykjanes peninsula extending into Reykjanes ridge. Scattering was detected on the ridge with sonar instruments [7], this scattering could indicate that there are some hydrothermal vents in the area. Precise locations where the bubbles were found are shown on Figure 5 [6]. It is now known that Reykjanes peninsula has a high capacity for geothermal resource and with the information regarding the bubbles and the seismic activity along the ridge it is estimated that geothermal energy could be found on the Reykjanes ridge as well.

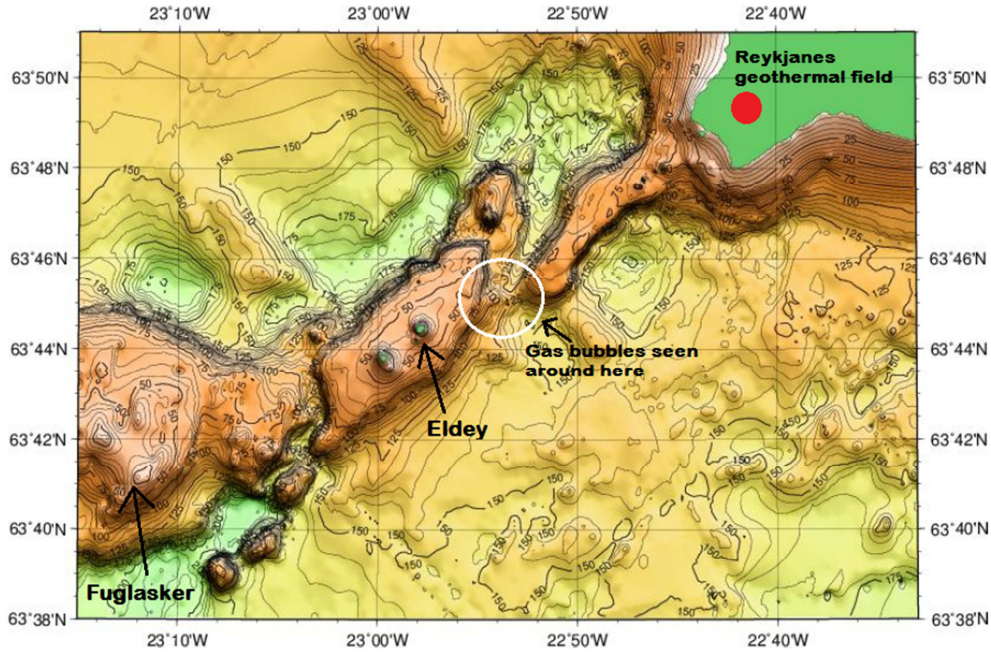

Figure 5 Showing where the gas bubbles were found in the Reykjanes ridge [8]

2.2.2. Conditions

The weather conditions at Reykjanes are not the optimal weather conditions for an offshore project and therefore it could be very difficult to operate offshore geothermal power plants there. The main reason for that are strong winds and high waves. The oil industry on the other hand has shown that the oil platforms have been operated at worse weather conditions than in Reykjanes. For that reason bad and windy weather in Reykjanes should not necessarily be an obstacle for future offshore projects. In Reykjanes the wind can go up to 40 m/s and the ocean current around Reykjanes is close to zero velocity at the surface and it is estimated to be around 2-3 m/s at 150 to 250 meters depth [9]. The waves can also be high on the Reykjanes coastline and that could affect the platforms structural calculation when it comes to choosing the foundation for the actual platform. Figure 6 shows how the current flow is around Iceland.

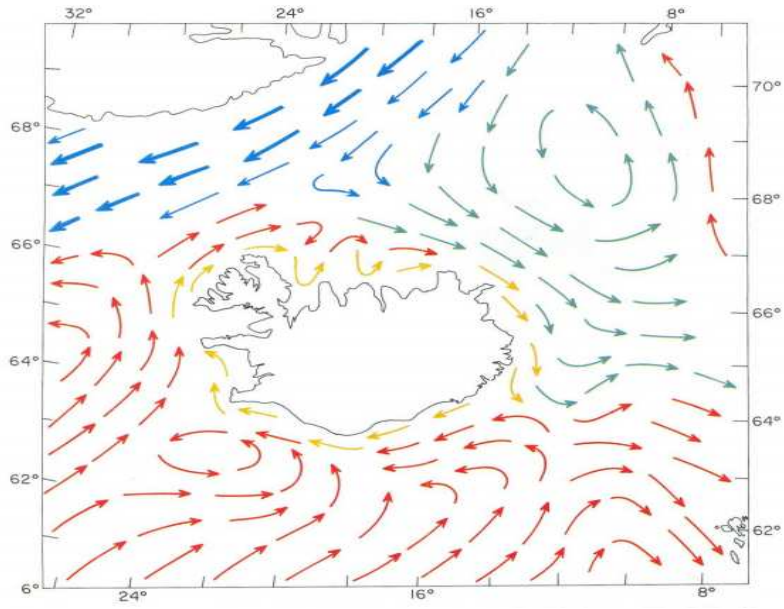

Figure 6 Ocean currents around Iceland

2.3. By-Products from Reykjanes Ridge

The geothermal area at Reykjanes is the only one place where the Atlantic ridge is seen on land, information collected from that area could therefore be compared to other hydrothermal vents coming from the ocean ridges. The hydrothermal vents often found near ridges are sometimes called black smokers. A research has been done where the topic was Reykjanes area and the samples were collected from a borehole at the depth of 1500 meters [10]. At that depth the pressure is so high that the geothermal fluid still has not started to evaporate even if the temperature of the fluid is over 300°C. Because the fluid was collected before it evaporates it shows the geothermal fluid before mixing with other materials like basalt. When the geothermal fluid was analyzed it showed that the metal content of the fluid was; iron (Fe) 9-140 ppm, copper (Cu) 14-17 ppm, zinc (Zn) 15-27 ppb, lead (Pb) 120-290 ppb, gold (Au) 1-6 ppb and silver (Ag) 28-107 ppb. These metals dissolve in other materials and they became part of precipitation within the pipelines. The question would be if it might be profitable to extract the metals with some kind of treatment. Although for now the precipitation is being thrown away as the power station company HS-Orka has not considered it feasible to extract the metals from the precipitation [10].

2.4. Offshore Drilling

2.4.1. Known Information

Drilling at the ocean crust is not a new method, in fact it has been done for decades within the oil industry as well as for geological explorations. The Reykjanes coast has the average ocean depth of 200 meters down to the ocean bed. The ridge area is known to be highly active with a heat flow into the ocean [2]. As shown on Figure 7 the seismic areas are very close to land and at feasible depth when it comes to drilling and operation. The red dots on Figure 7 show seismic activity. The activity is most intense around Fuglasker, but even closer to land it looks promising as well as seismic measurements indicate that there could be heat stored beneath.

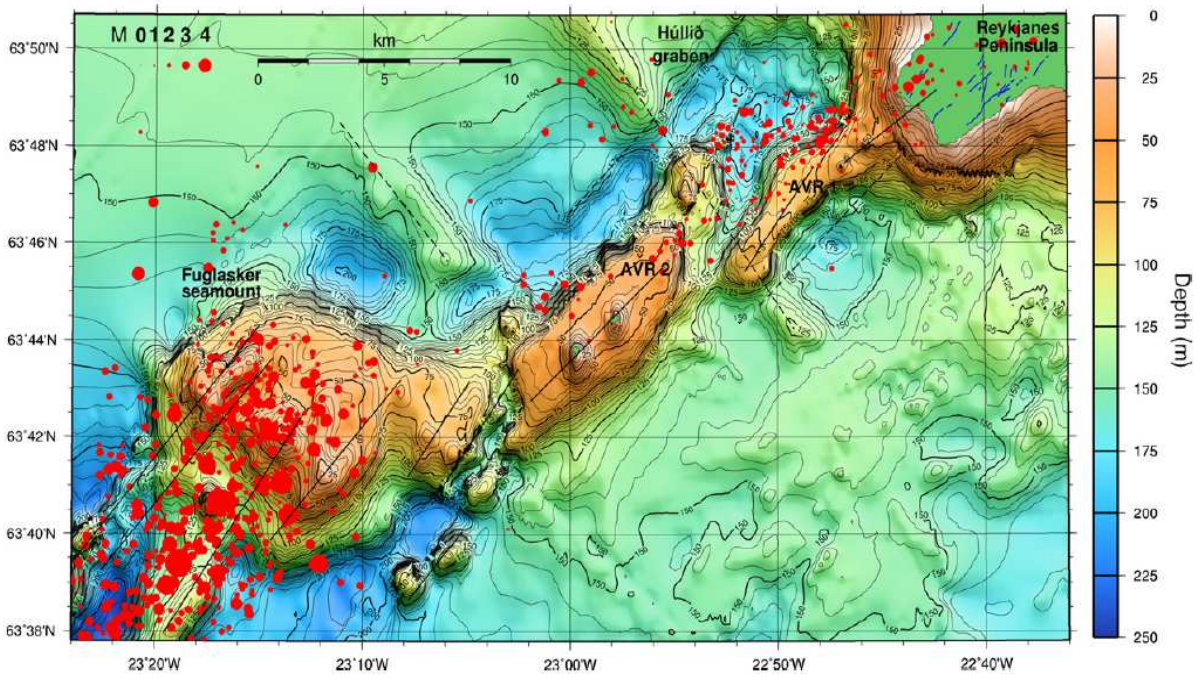

Figure 7 Map showing the Reykjanes ridge seismic activities between 1990 and 2004 [2]

The ocean depth on Reykjanes ridge is similar to the gas production area located in the Barents Sea north of Norway called “Snøhvit”. That area has a depth to the seabed between 250 to 340 meters and a distance to shore of 140 km [11]. The boreholes are mostly extracting natural gas and the stations around the boreholes as well as the pipe collecting systems are all underwater, see Figure 8.

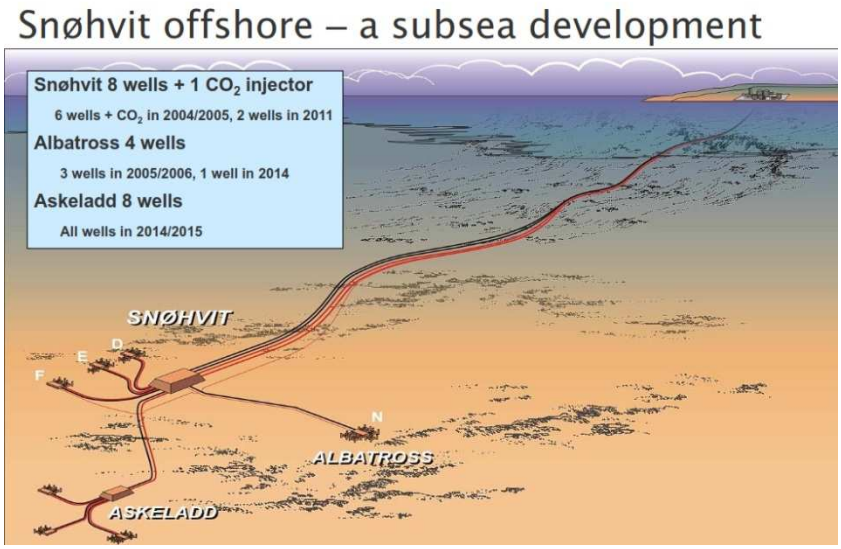

Figure 8 Snøhvit area [11]

The drillings for Snøhvit area were done with a drilling vessel from a company called Transocean [12]. They drilled eight oil production wells and one CO_2 injection well. All of those wells are connected with underwater pipeline system and natural gas is pumped to an island where it is processed before it is transported with a transport vessel to its destination [11]. The drilling vessel is shown on Figure 9.

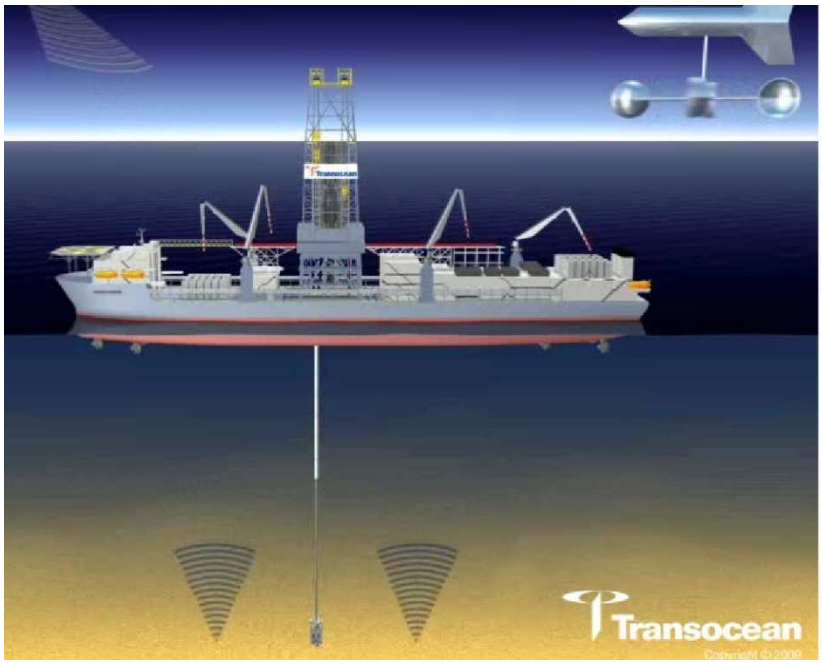

Figure 9 Drilling vessel from Transocean [12]

2.4.2. Drilling Technology

The technology for offshore drilling has the same principles as drilling on land [13]. That is using rotary drilling rig offshore and onshore. The average drilling depth is approximately 100 meters per day. The energy transmitted to the drill bit comes from several forces; the downward force from the weight of the drill string, the rotation driven from the top drive and the fluid flow of the mud which keeps the rock bit clean from any cuttings coming from the drilling [14].

When drilling from a vessel similar methods are used as on land, e.g. the cooling system using water or mud for a working fluid while the drilling is the same. The mud system is also used to get the cuttings away from the drill bit as well as to bring the cuttings to the surface. The cuttings are then analyzed to estimate the temperature of the fluid and geological mapping for the drilling area. The cuttings are taken out of the circulating system in the mud cleaning unit shown on Figure 10 and described in more details in section 2.4.4.

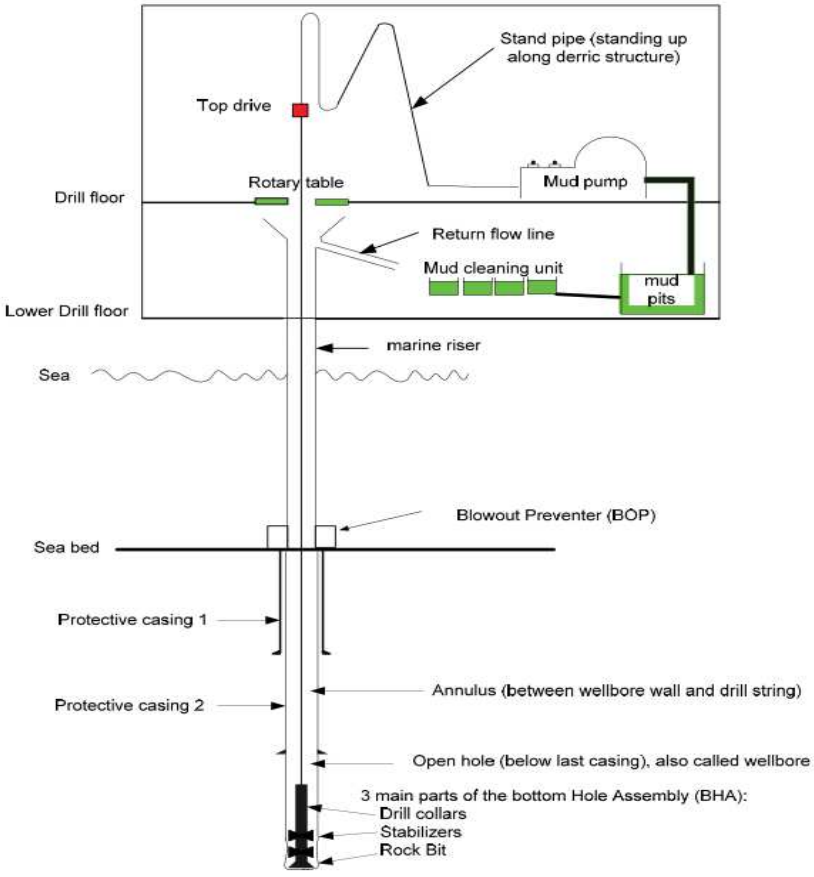

Figure 10 Offshore drilling process circle [14]

2.4.3. The Casing System

The main feature for a high temperature well is the casing. The casing typically consist of three cemented casing strings; surface casing which is the top one and typically between 60-90 meters, the anchor casing which is the middle casing typically between 200-400 meters, and the production casing typically between 600-1000 meters. After the production casing comes the liner typically between 800-2000 meters. The liner is usually perforated and that is done to enable the geothermal fluid to flow into the casing and towards the wellhead. In some cases where the ground is stable no liner is needed.

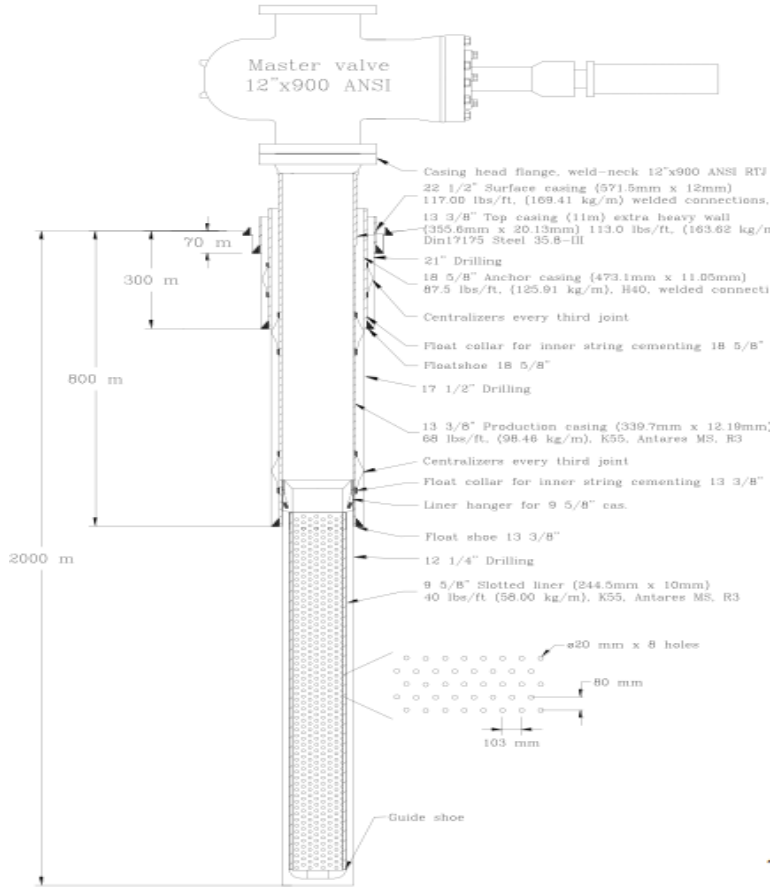

Figure 11 Geothermal casing design [15]

There is usually a size difference in the casing diameters depending on if casing is done for oil production well or geothermal production well. The typical diameter for the oil production casing well is 180 millimeters and the typical diameter for the geothermal production casing is 245 millimeters [15]. The main reason for casing the well is to block unwanted liquid that might be at lower temperature than the expected geothermal fluid, to have safer drilling by installing each casing after the depth is reach, to support the well and to anchor the wellhead for controlling. Further details are shown on Figure 11.

2.4.4. The Mud System

The mud is in a closed working cycle. It goes through the mud pumps and down into the drill string and through the nozzle of the drill bit. After the mud has gone through the drill bit it goes back up through the annuals and into a cleaning processor which cleans the cuttings from the mud and returns it into the mud tank where it is then pumped back into the system [14]. This process can be visualized on Figure 10.

When using mud in offshore situations more care is needed than for on land situations e.g. it is recommended that the mud does not go under a designed mud temperature. If that occurs the mud has the tendency to hydrate and the mud viscosity increases. Hydrate formation is a well-known problem in under water drilling. A hydrate forms in water environment where the mud pressure increases and the mud temperature decreases. A hydrate forms when molecules from one substance enclose within the crystals of another molecule [14]. The mud viscosity increases with lower temperature. The mud viscosity has to be as stable as possible so it will perform the way it should, e.g. to bring the cuttings up to the surface for further analysis [14]. When drilling for the liner part in geothermal drilling, water is usually used instead of mud. That is done because the mud has the tendency to close the cracks where the geothermal fluid is coming from.

2.4.5. Wellhead

After the drilling a wellhead can be installed. The oil wellhead in Norway should be installed according to an offshore standard i.e. the Norwegian standard Norsok [16]. Norsok standard is used in all offshore oil projects in Norway. It is considered that a similar wellhead can be used for offshore geothermal as for oil/gas although the temperature is far from being the same in both cases.

The wellhead can be in the form of a subsea wellhead, such wellheads are more expensive than ordinary wellheads both in installation and maintenance. The control system for the wellhead has to be a remote control, controlled from land [16]. Where the wellhead is located on a platform and therefor above the ocean an ordinary geothermal wellhead can be used as there is no need for an expensive subsea wellhead.

2.5. Technical Information for Reykjanes Area

2.5.1. Known Information

The Reykjanes steam field area is estimated to be around one square kilometer if measurements were done from visible steam signs at the surface [17]. Resistivity measurements indicate that the area is at least four times greater than the above measurements and extends into the ocean to the southwest part of the peninsula. To visualize the location see Figure 12, the red dot shows the location of Reykjanes power plant [17].

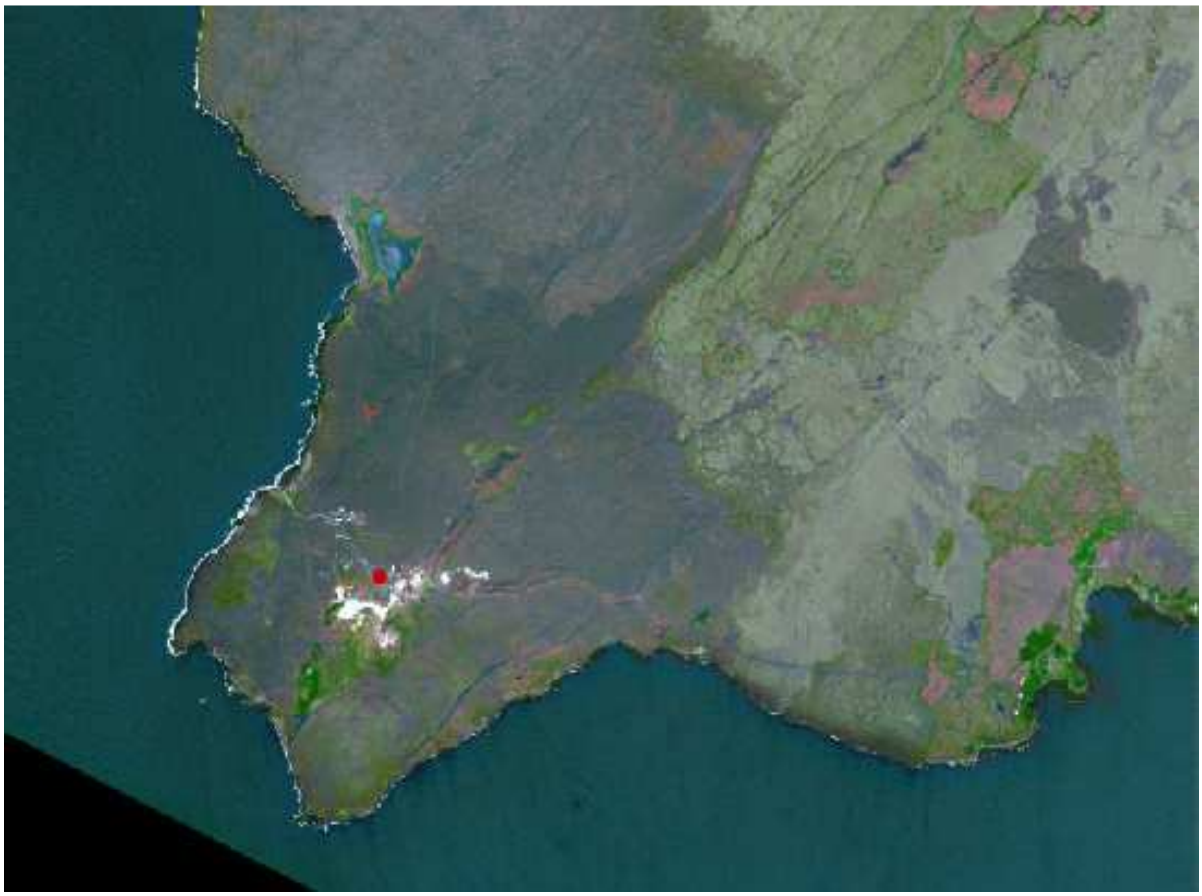

Figure 12 Reykjanes peninsula, rod dot on map shows the location of the Reykjanes power plant [18]

The Reykjanes geothermal steam field is mostly covered with lava and is one of the most studied geothermal fields in Iceland. The foundation for these researches reaches back to the years before 1970 as seismic activities occurred frequently in the area [17]. Reykjanes steam field has the highest temperature of steam fields in Iceland, and it has been used for power production for over 30 years without significant impact on the reservoir [17]. The liquid that is available and is used for energy production consist mainly of salt water [17].

For the Reykjanes steam field, wells have been drilled and monitored and for many years data has been collected; e.g. measurements of mass flow, pressure and enthalpy [19]. The production wells are shown on Figure 13

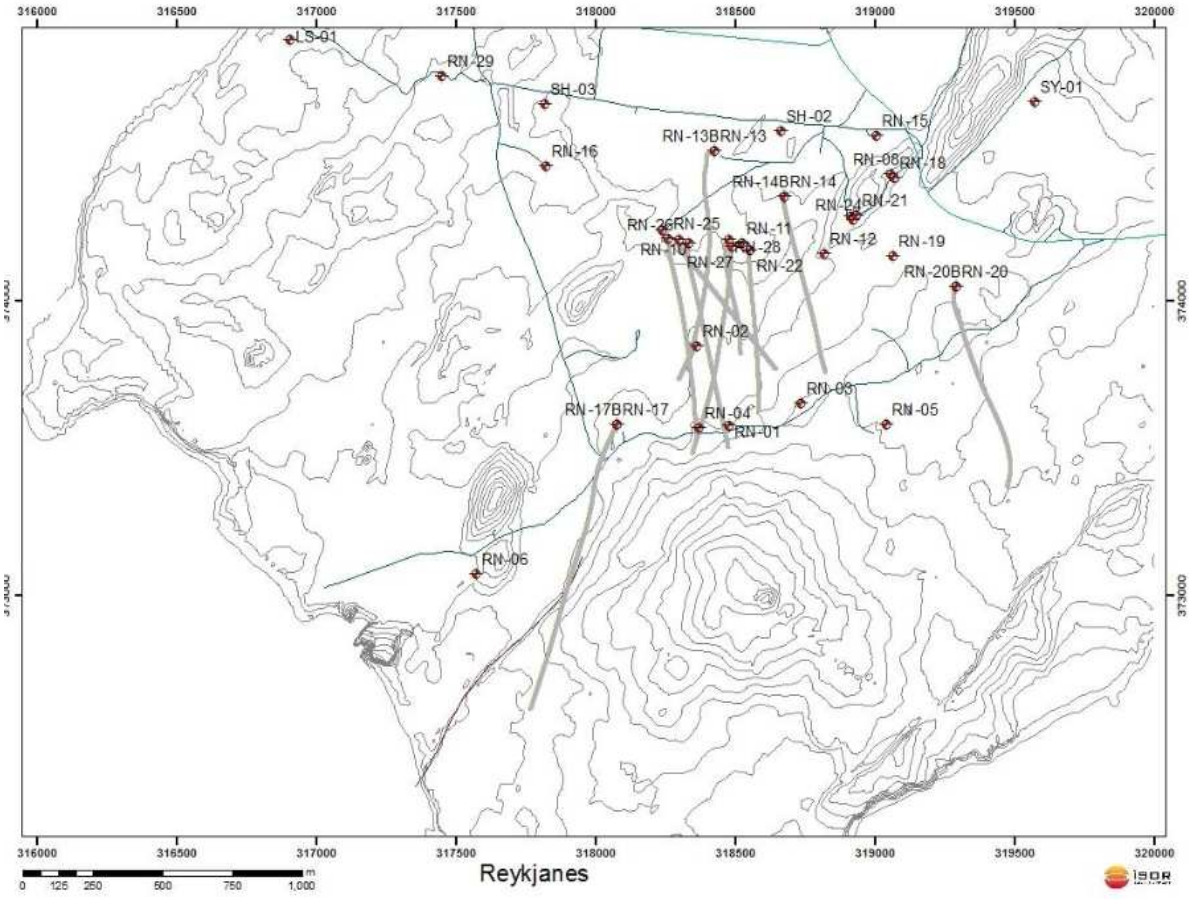

Figure 13 A figure showing the location of the production wells on the Reykjanes peninsula [20].

3. Method

The power outputs are calculated for three energy processes; three types of single flash cycles, an organic Rankine cycle and thermoelectricity. The calculations give potential net power output for each scenario described in section 4. Calculations for the single flash power cycle are done in EES and are shown in appendix 3. For the binary cycle, the selection of the working fluid is analyzed to evaluate which one gives the best power output for the given condition. The components for the cycles are considered to be similar. The thermoelectricity calculations are done in Matlab and are shown in appendix 5. The power cycles processes are assumed to neglect heat loss and change in the kinetic and potential energy as well as neglecting non-condensable gas (NCG).

3.1. Data Analyzed

The boreholes analyzed are the boreholes used by the Reykjanes power plant as those boreholes are close to the Reykjanes ridge area and therefore assumed to have similar properties. Information gathered from the Reykjanes boreholes was then used for further analysis. The actual data for the boreholes located on the Reykjanes peninsula were collected from two companies; ISOR (Icelandic Geosurvey) and HS Orka (the owner of the steam field). From ISOR, information about the productivity curves for the boreholes was collected and analyzed. Power production and enthalpy information was collected form HS Orka. The boreholes are shown on Figure 13 and in appendix 1.The productivity curves used in this research where simulated from all the production curves available from the data bank listed in appendix 1. The production curves for each borehole were plotted from the data referring to the same appendix and are shown on Figure 14

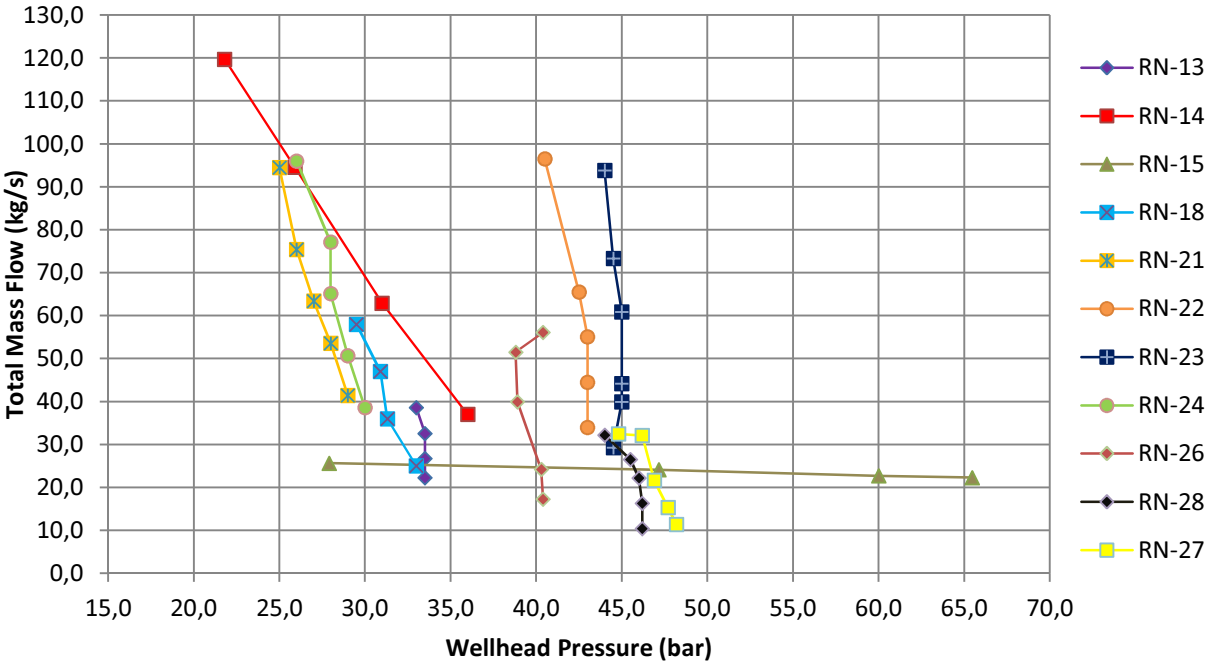

Figure 14 Plotted production curves from Reykjanes steam field

With information from all the individual production curves a simulation was performed with the calculation software Matlab. Matlab was used to make a hypothetical production curve resembling the most realistic production curve. The actual power output was calculated using this hypothetical average production curve.

To calculate the average production curve, calculations of the mean and standard deviation for the well parameters were needed, those calculations were performed in Excel and are shown in Table 1.

Table 1 The mean and the standard deviation of the cutoff pressure, enthalpy and the mass flow from the production curves shown on Figure 14

Parameter	Mean, μ	Standard deviation , σ
Pressure [bar]	36,2	8,4
Mass Flow [kg/s]	48,1	25,35
Enthalpy [kJ/kg]	1570	364,5

The equation to find the mean is expressed with the formula:

$$\mu = \Sigma x / n \quad (1)$$

Where μ is the mean, ∑x is the sum of all fixed numbers gathered from the data collected and n is the quantity of the fixed numbers.

The equation to find the standard deviation is expressed with the formula:

$$\sigma = \sqrt{[\sum(x_i - \mu)/n]} \quad (2)$$

Where σ is the standard deviation, x_i is each fixed number gathered from the data collected, μ is the mean calculated using equation 1 and n is the quantity of the fixed numbers.

3.1.1. The Average Production Curve

The average production curve was calculated and simulated by generating one hundred wells, where the probability follows the normal distribution parameters from Table 1, see Matlab code in appendix 2. The average well flow for these 100 wells is then plotted against wellhead pressure, and a regression curve fitted. This process was then repeated a few times, with similar results. The regression curve is shown on Figure 15 together with a sample of the 100 well average generated. The regression curve was then used in the program EES to determine the optimal pressure and flow rate that will enter the turbine for the power production options used for the calculations in section 4. This was done to maximize the power output from the power cycles.

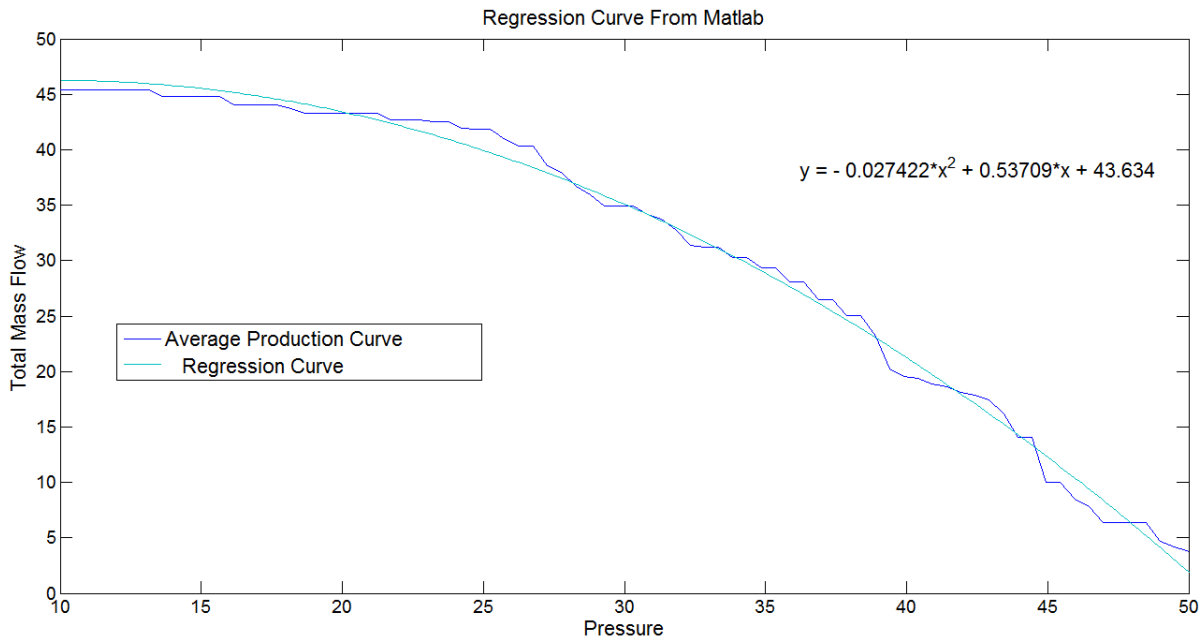

Figure 15 Regression curve used for the productivity curve

3.2. Energy Conversion

As previously stated, the following energy processes and power cycles were analyzed:

Single flash power plants on a platform in the ocean, land based power plant with a separator at the ocean bed, underwater power plant, binary power plant located on land with a heat exchanger on the ocean bed and thermoelectricity device producing electricity using temperature difference between the ocean and the geothermal fluid. In the next sections these processes are described generally and the theoretical groundwork for the calculations introduced.

3.2.1. Single Flash Systems

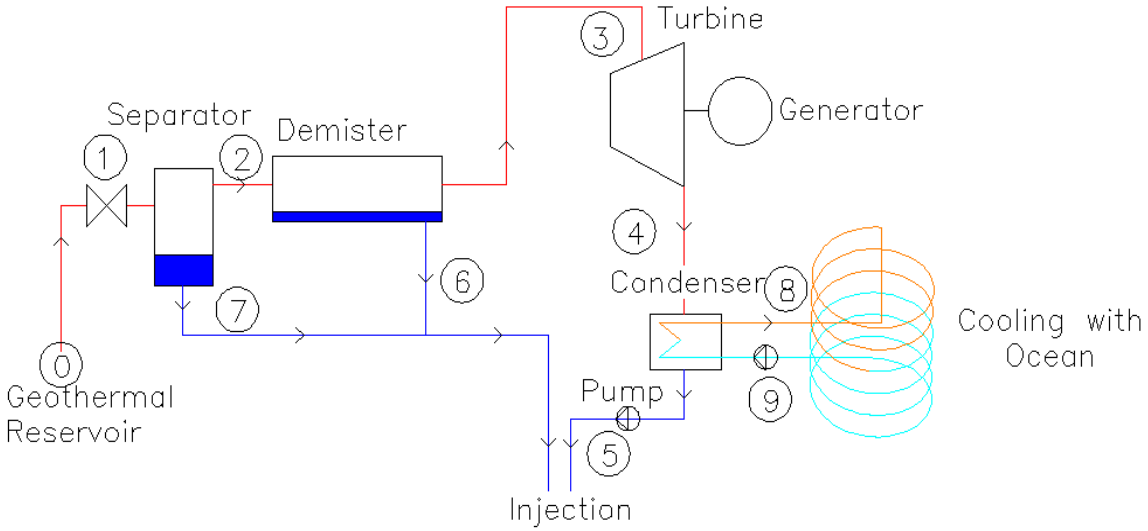

Figure 16 Process diagram of a single flash cycle

A single flash system is the most widely used power cycle in electrical geothermal power plants and accounts for approximately 32% of installed geothermal power plants, those are estimated to produce 42% of the power produced from geothermal energy worldwide [21]. Single flash power cycles are considered optimal when the temperature of the geothermal reservoir is above 190°C [21] as shown in Lindal diagram on Figure 17. When utilized, the geothermal fluid flow coming from the reservoir at state 0 on Figure 16 is flashed at the wellhead at state 1 and directed to a separator where it is separated into steam and water. The steam at state 2 is then directed to the demister to remove the last droplets before entering the turbine at state 3. In the turbine the energy from the steam rotates the turbine blades producing mechanical energy, which is then transformed into electricity with a generator [22]. The steam

at state 4 is then condensed in a condenser into liquid form at state 5. When using a condensing turbine, the pressure for the steam exhausting from the turbine is usually around 0,1 bar absolute [21]. The purpose for using a low pressure turbine unit is to maximize the power output since more energy is converted to electrical power by lowering the turbine exhaust enthalpy. The power output equation is shown in section 3.2.7. The condenser needs to have external flow for cooling down and condensing the geothermal liquid. Since the process described in this project is considered to be close to the ocean it was decided to use ocean water for the condensation process. After the steam is condensed into liquid form it is mixed with the separated water at state 6 and 7 and re-injected into the geothermal reservoir.

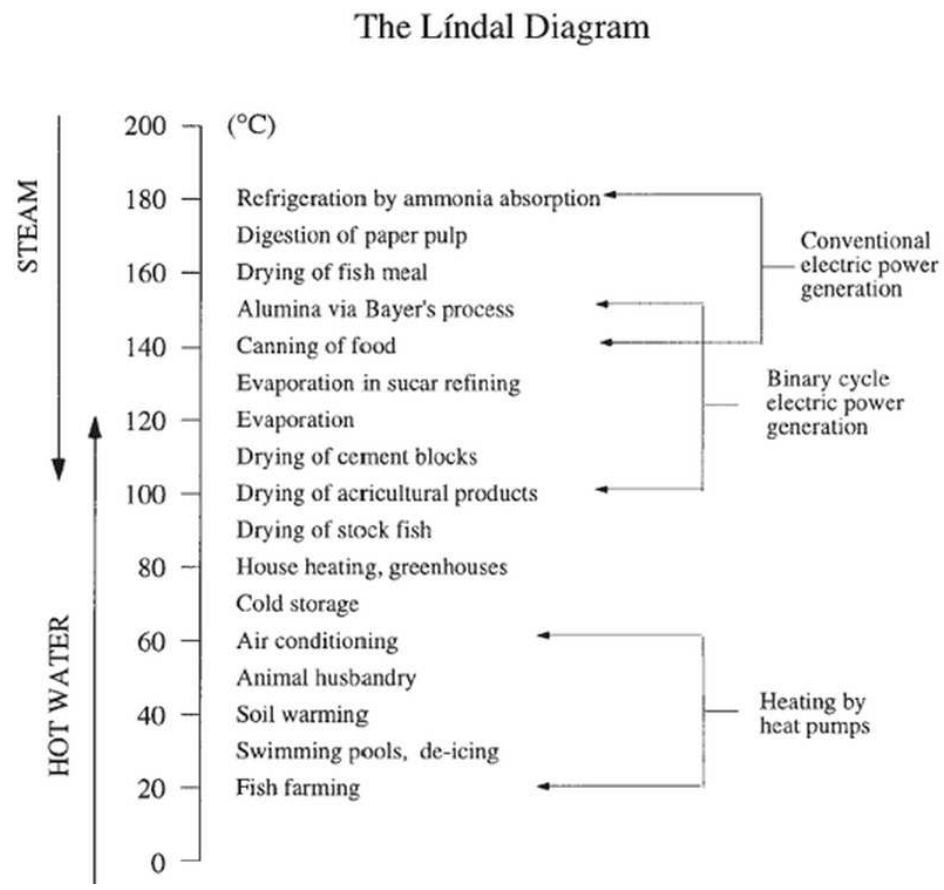

Figure 17 Líndal diagram showing utilization of geothermal energy at different temperatures [23]

3.2.2. Energy Conversion Processes for Single Flash

The energy conversion process describes how the single flash processes are implemented with regards to the components used at each state. The geothermal fluid undergoes a transition from being at saturated liquid phase to a condition of being at saturation vapor phase.

3.2.3. Temperature-Entropy Diagram for Single Flash

A typical temperature entropy diagram for the steam process is shown on Figure 18. The same figure can be resampled in the results section as it shows the actual thermodynamic state of the geothermal fluid used for calculations. Following subsections 3.2.4 to 3.2.8 show the governing equations for each process within the overall single flash system.

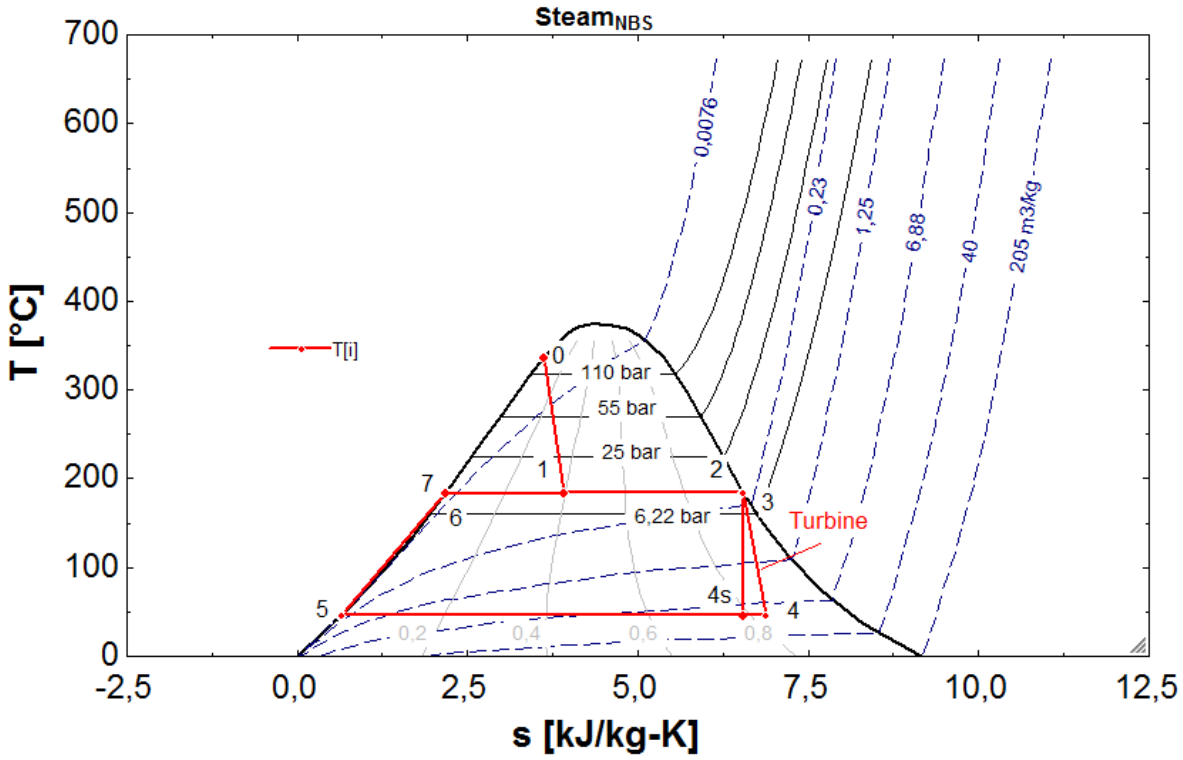

Figure 18 Temperature - entropy diagram for single flash

3.2.4. Flashing Process

The geothermal fluid at state 0 is a single phase liquid at saturated pressure. The fluid is flashed between state 0 and 1 and down to calculated optimal pressure P_1. As this system is calculated as an isenthalpic process and neglecting thermal loss in pipelines and change in the kinetic and potential energy we can assume that there will be no change in enthalpy. That is:

$$h_0 = h_1 \tag{3}$$

3.2.5. Separation

The first major component in the power plant is the separator. Separators are used to separate two phase flow into two individual one phase flows of liquid and steam. Coming out of the separator the quality of the steam is to be x=1, that is 100% steam and for the separated water

it is x=0, that is 100% liquid. The equation to find the steam quality is expressed with the formula:

$$x_1 = \frac{h_1 - h_7}{h_2 - h_7} \tag{4}$$

Where h_2, h_3 and h_7 refer to the enthalpy of the fluid at states 2, 3 and 7 respectively. With that information and referring to Figure 16 where the separator is at state 1, the separation of the steam going in at state 3 and the separated water going out at state 7, a calculation for the mass flow going towards the turbine is expressed with the formula:

$$\dot{m}_2 = \dot{m}_1 * x_1 \tag{5}$$

3.2.6. Demister

The second major component is the demister. The demisters job is to take the last droplets if any away from the steam that will be entering the turbine. Those precautions are done to protect the turbine from any remaining droplets, if droplets find their way into the turbine, it could damage the turbine blades dramatically. A demister is considered to be at its best performance when the distance from the separator is around 500 meters [24]. There are calculations in the EES code regarding how much separated water the demister collects, the code can be found in appendix 3.

3.2.7. Turbine Expansion

The most important component is the turbine. Many producers offer turbines and turbines are usually custom designed for each project [25].

The expansion through the turbine gives the actual work and is shown between state 3 and 4 on Figure 16. The actual work is determined by the steam mass flow after the separator and the difference in enthalpy through the turbine. The efficiency of the turbine is usually given from the turbine producer, in this case the efficiency is set to 0,85 [25]. The isentropic efficiency η_s is the ratio of the actual work and is calculated with the equation below:

$$\eta_{turbine} = \frac{h_3 - h_4}{h_3 - h_{s4}} \tag{6}$$

Where h_{s4} is found as a function of P_4 and S_4. When the enthalpy of the fluid exiting the turbine is found the turbine power output is:

$$\dot{W}_{turbine} = \dot{m}_3 * (h_3 - h_4) \quad (7)$$

Where $\dot{m}_3$ is the mass flow of the steam and h_3 and h_4 are the enthalpies before and after the turbine.

The generator is estimated to have the efficiency of 0,95 [25]. The generator output is calculated with the formula:

$$\dot{W}_{generator\ output} = \eta_{generator} * \dot{W}_{turbine} \quad (8)$$

3.2.8. Condensation

The condenser is the fourth major component and its job is to condense the fluid coming from the turbine. The fluid exiting the turbine is a mixture of steam and liquid and is expressed with the formula:

$$x_4 = \frac{h_4 - h_{f4}}{h_{g4} - h_{f4}} \quad (9)$$

Where h_4 is the enthalpy of the fluid exiting the turbine, h_{f4} is the saturation liquid enthalpy of the fluid exiting the turbine and h_{g4} refers to the saturation vapor enthalpy exiting the turbine.

In the condenser the heat from the condensing fluid is rejected into a cooling fluid, which in this project is considered to be ocean water, and the two fluids (geothermal steam and ocean water) are not mixed together. The condensation is shown between state 4 and 5 on Figure 16. Calculation of the thermal heat $\dot{Q}_{out}$ rejected from the cycle is expressed with the formula:

$$\dot{Q}_{out} = \dot{m}_3 * (h_4 - h_5) \quad (10)$$

The required flow for the cooling side of the condenser can be expressed with the energy balance formula:

$$\dot{m}_9 * (h_8 - h_9) = \dot{m}_4 * (h_4 - h_5) \quad (11)$$

The require pump work used for cooling is then calculated with the formula:

$$\dot{W}_{cooling,pump} = \frac{\dot{m}_{ocean} * g * H_{total\ head}}{\eta_{pump}} + \frac{v_{water} * (P_9 - P_8)}{\eta_{pump}} \quad (12)$$

Where g is the gravitational acceleration, $H_{total\ head}$ is the overall height distance between the pump and the ocean, v_{water} is the specific volume of the water and $(P_9 - P_8)$ is the pressure difference between the inlet and outlet for the pump.

3.2.9. Exergy Efficiency

The exergy efficiency is the efficiency that compares the maximal power output from the power plant to the maximal theoretical power output that the geothermal fluid could theoretically give. The exergy efficiency is expressed with the formula:

$$\eta_{exergy} = \frac{\dot{W}_{net}}{\dot{E}} \tag{13}$$

Where W_{net} stands for net power output and E stands for exergy energy that is calculated with the formula:

$$\dot{E} = \dot{m}_1(h_1 - h_{ds} - T_{ds}(s_1 - s_{ds})) \tag{14}$$

Where $\dot{m}_1$ is the total mass flow, h_1 is the enthalpy in state one, h_{ds} is the dead state enthalpy where ds stands for dead state and is the environmental condition at the calculated location, T_{ds} is the ambient temperature, s_1 is the entropy at state 1 and s_{ds} is the entropy at dead state found with ambient temperature and pressure.

3.2.10. Pipe Sizing

The pipe sizing is an important factor when it comes to the power plant design and can have major impact on the economic side of each project. The minimum pipe inner diameter, D, is calculated with the formula:

$$D = \sqrt{\frac{4 * \dot{m}}{\pi * v * \rho}} \tag{15}$$

Where $\dot{m}$ is the mass flow rate, v is the velocity and ρ is the density of the fluid flowing through the pipe. When the inner diameter has been found, a commercial pipe size is found as the next pipe diameter size available. The required thickness for the pipeline is calculated with the formula:

$$t_m = \frac{P_{design} * D_o}{2(SE + P_{design} * y)} + A \quad (16)$$

Where t_m is the minimum wall thickness measured in meters, P_{design} is the design pressure in bars, D_o is the outside diameter in meters, SE is the material allowable stress in bars, y is the material dependent coefficient and A is the additional thickness i.e. if needed because of corrosion [26]. The thickness can also been determined from annexes all after pipe geometry and its use.

3.2.11. Pressure Loss

Pressure loss is one of the main concerns in steam gathering systems, because in some cases the pressure loss has a direct influence on the power output, e.g. if the enthalpy of the steam entering the turbine decreases with decreasing pressure (increasing pressure loss) in the pipelines directing the steam to the turbine. The major factors affecting pressure loss are the pipe roughness, density of the fluid, pipe length, mass flow rate (fluid velocity) and the geometry of the pipe line which is the most critical factor [21]. The friction factor could be calculated after the Colecrook and White formula:

$$\frac{1}{\sqrt{f}} = -2.0\ log\left(\frac{e/_D}{3.7} + \frac{2.51}{Re\sqrt{f}}\right) \quad (17)$$

Where f is the friction factor and is dimensionless, e is the inner roughness factor measured in meters, D is the inner diameter measured in meters and Re is the Reynolds number and is dimensionless. The Reynolds number formula is:

$$Re = \frac{(V * D * \rho)}{\mu} \quad (18)$$

After calculating the friction factor f the pressure loss for one phase flow can be calculated with the formula:

$$\Delta P = \rho g f * \frac{L}{D} * \frac{V^2}{2g} \quad (19)$$

Where ρ is the density of the fluid, g is the gravitational acceleration, L is the length of the pipe, V is the fluid velocity and μ is the fluid dynamic viscosity.

3.3. Binary Cycle System

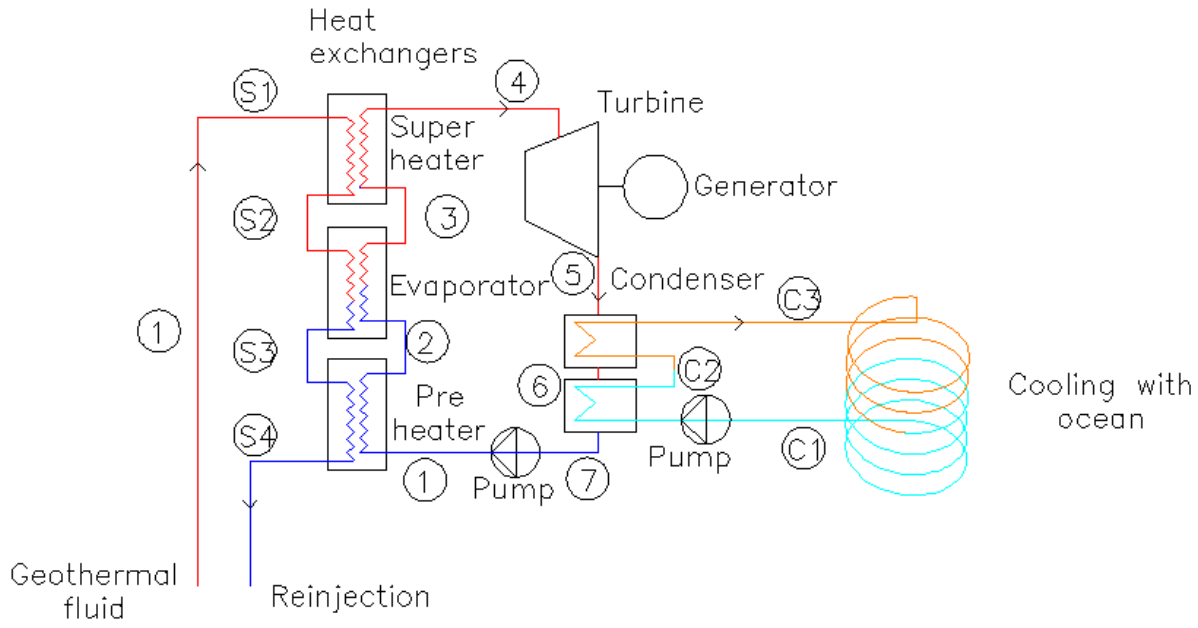

Figure 19 Process diagram of a binary cycle

Binary cycles are commonly used for power production when the temperature of the geothermal fluid is lower than 150°C [21] and is shown in the Líndal diagram on Figure 17. Binary plants operate with heat exchangers where the hot brine (geothermal fluid) passes through the heat exchanger at states S1 to S4 shown on Figure 19 and the energy from the brine boils the working fluid at state 2 to 3 on the other side of the heat exchanger. The working fluid is selected so it evaporates at a different temperature than the geothermal fluid and it all depends on the actual temperature of the geothermal fluid. The working fluids selected for geothermal applications can e.g. be isobutene, methanol or other fitting each case. After vaporizing the working fluid in the heat exchanger the fluid is directed into the turbine at state 4, where it spins turbine blades and produces mechanical energy. The energy is then transformed into electricity with a generator as for the single flash process described in section 3.2.7. The fluid is then condensed like described in section 3.2.8 and pumped back to the heat exchanger for reheating in states 5,6,7 and 1. The geothermal fluid is then re-injected into the reservoir at state S4.

3.3.1. Energy Conversion Processes for Binary Cycle

The energy conversion process describes how the binary process is implemented with regard to the components used at each state. The working fluid undergoes a transition from being at high saturation liquid temperature, pressure and enthalpy to a condition being at saturation vapor temperature, pressure and enthalpy. It is not the same for all working fluids e.g. isopentane and isobutene are in a supercritical state when going through the turbine.

3.3.2. Temperature-Entropy Diagram Binary

A typical temperature-entropy diagram for the methanol process is shown on Figure 20. The same figure can be resampled in the results section as it shows the actual thermodynamic state of the working fluid used for calculations. Following subsections 3.2.4 to 3.2.8 show the governing equations for each process within the binary system.

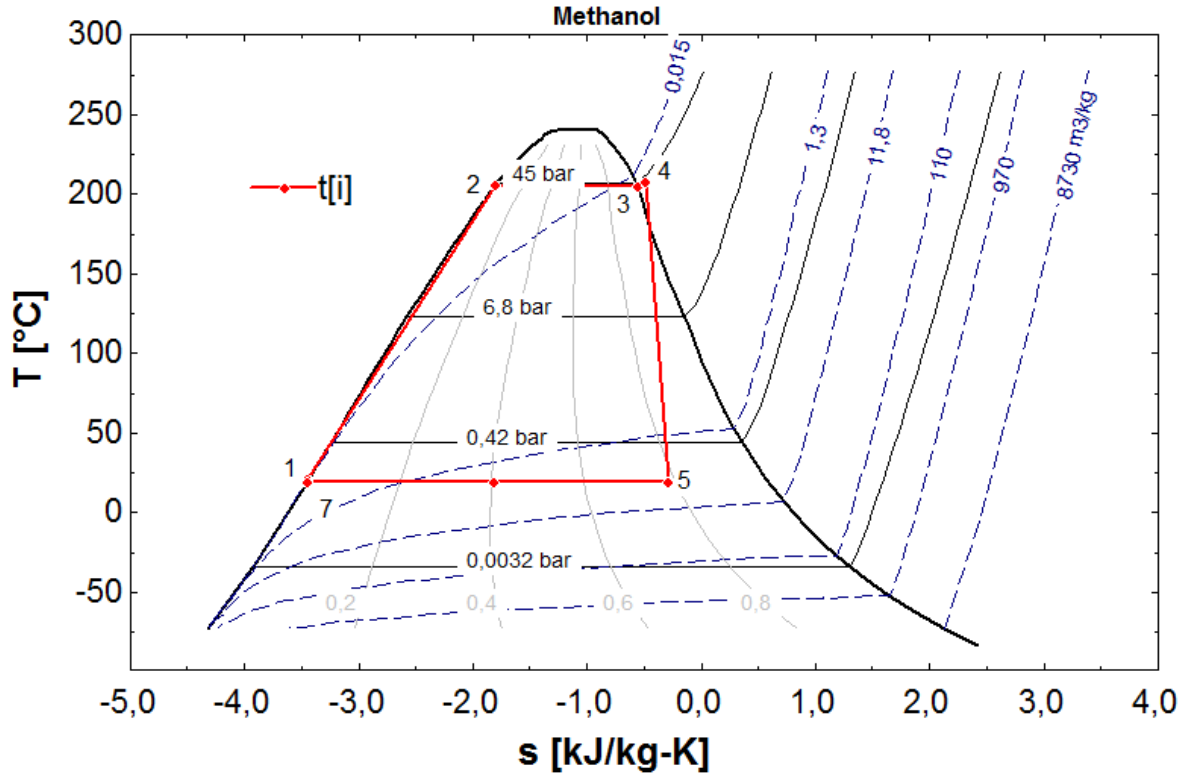

Figure 20 Temperature - entropy diagram for binary cycle calculation with methanol as the working fluid

3.3.3. Component Analysis

The component analysis has the same principles as the single flash component analysis described in section 3.2.1. We can consider the turbine expansion, condensation process and the cooling pump to be the same principles in both cases.

3.3.4. Heat Exchanger for a Binary Process

A heat exchanger is used to exchange heat from one fluid to another fluid. The way to exchange heat from one fluid to the other is to have the fluids move in the same or opposite directions. As written in the process description the process is assumed to be isenthalpic, neglecting heat loss from the pipelines and heat exchanger as well as neglecting change in the kinetic and potential energy. Non-condensable gas (NCG) content in the geothermal fluid side of the heat exchanger is neglected as well. The energy balance equation for the heat exchanger is:

$$\dot{m}s_1(h_{s1} - h_{s3}) = \dot{m}_{wf}(h_4 - h_2) \tag{20}$$

Where $\dot{m}s_1$ is the geothermal mass flow and $\dot{m}_{wf}$ is the working fluid mass flow. The h is the enthalpy marked with its position as a subscript. The heat exchanger is divided into three heat exchangers which are the preheater, the evaporator and the super-heater. The preheater as the name indicates preheats the binary fluid to the saturated liquid curve in state 2 on Figure 20. The evaporator evaporates the fluid to saturated vapor curve in state 3, and the super heater is used to superheat the steam two degrees above the saturated vapor curve. This is done to avoid liquid droplets entering the turbine, and can be done simply by having some of the heat exchanger surface above the liquid surface in the vaporizer, thereby functioning like a small super-heater The pinch for the exchanger is set to be 3°C [25]. That is the average pinch used in Europe [25]. The pinch is defined as the smallest temperature difference between the fluids in the heat exchanger. The lower the pinch is the bigger the heat exchanger needs to be. To estimate the actual pinch for each case, profitability calculations are needed to calculate the most profitable economic model for any given situation.

3.3.5. Circulation Pump in a Binary Process

In order for the working fluid to reach its pressure at the turbine inlet a feed pump is needed. The feed pump component in the process can be seen on Figure 19. As mentioned in section 3 heat transfer from the pump and kinetic and potential energy are neglected due to reasons explained in section 3. The pumps efficiency is set to be 0,65 [25]. The formula to calculate the actual work needed for the pump is expressed as:

$$\dot{W}_p = \frac{\dot{m}_{wf}(h_7 - h_1)}{\eta_{pump}} \tag{21}$$

3.4. Thermoelectricity

Thermoelectricity has been a known method for a long time for power production. The method used is often called the Seebeck effect. It comes from a German physicist named Thomas Seebeck. Thermoelectricity can be produced from temperature difference (ΔT) between two fluids. When one side is at different temperature than the other side, an electric current will flow in the circuit between the two sides producing electricity. The greater the temperature difference is the more current can flow in the circuit and therefore more electricity can be produced. Thermoelectricity could e.g. be used in rural places where ΔT conditions are optimal to power small equipment that would need small amount of electricity. Figure 21 describes the process more visually.

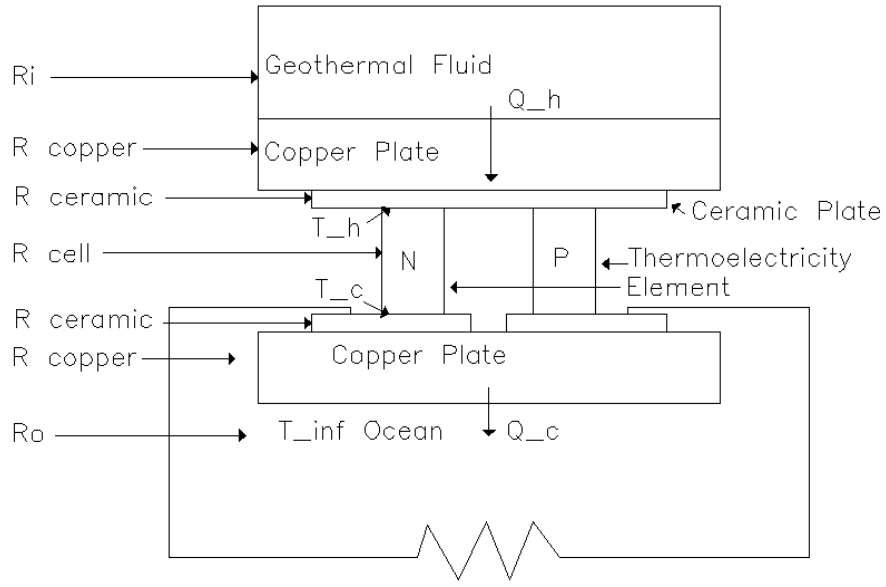

Figure 21 Single thermoelectric couple

Where $\dot{Q}_h$ is the thermal heat going through the cell, $\dot{Q}_c$ is the thermal heat after going through the cell, T_h and T_c are the temperatures on each side of the cell and N and P are the crystals in the cells, utilizing the temperature difference from the fluids to produce electricity. The crystals are made from mixing of the material Bismuth Telluride [27] and when the two conductors N and P have electric contact, electrons from one concoctor flows into the other conductor producing electricity. The materials used around the cells are different, all depending on the situation but copper is used as the metal between the fluids in the cell because of high thermal conductivity although detailed analysis are needed to see what metal fits the geothermal fluid best. The material used between the copper and the cell are ceramic plates and they are used as an electrical insulator. Figure 22 is a conceptual drawing of the

components with regard to each other and Figure 23 is a drawing describing the geometry for one square meter of thermoelectricity device as calculated here.

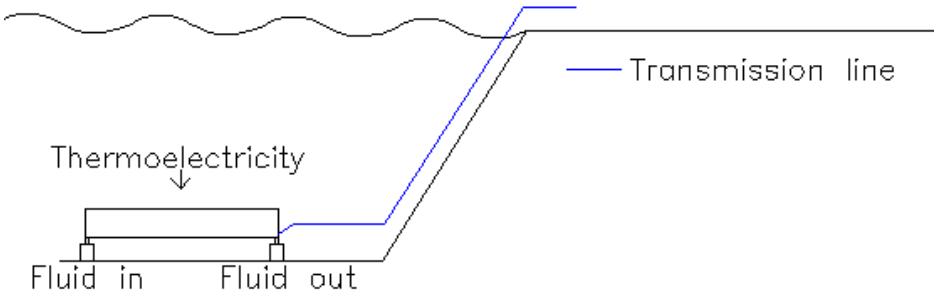

Figure 22 Conceptual drawing showing how the thermoelectricity power station could look like

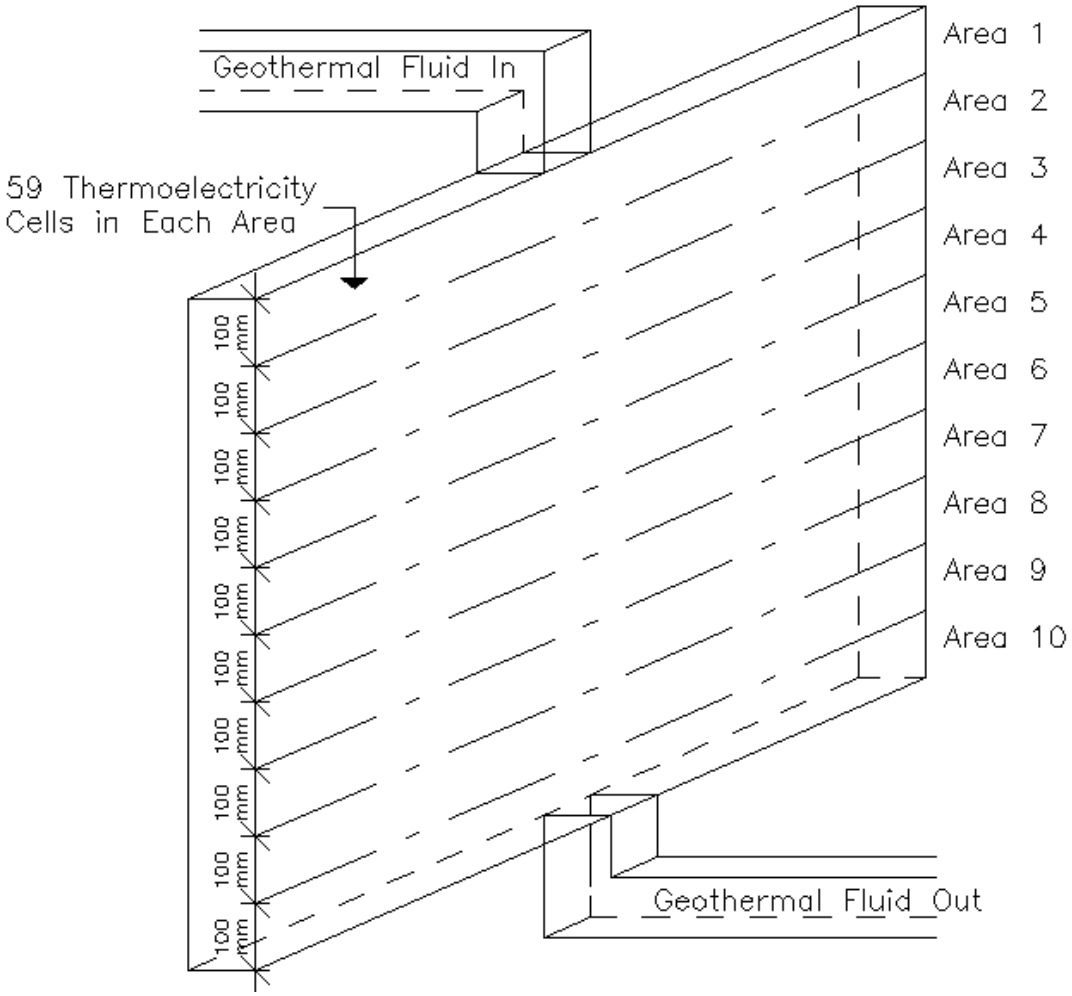

Figure 23 Drawing describing the geometry for one square meter of thermoelectricity device

The calculation for the thermal heat flow through one cell was done in Matlab. Most of the parameters needed to calculate the heat transfer trough one cell are gathered from heat

transfer book [28]. The thermal resistance for the geothermal fluid is expressed with the formula:

$$R_i = \frac{1}{h_i} \tag{22}$$

Where h_i is the convection coefficient of the inside media (in this thesis calculated for the geothermal fluid). The thermal resistance for the copper plate is expressed with the formula:

$$R_{copper} = \frac{L}{k} \tag{23}$$

Where L is the thickness of the copper plate used and k is the thermal conductivity for copper. The thermal resistance for the ceramic plate and the cell are expressed with the same formula as for the copper thermal resistance. Thermal resistance for R_o varies with the height of the device used for calculations and therefore calculations for several values are needed. Calculations for the R_o are expressed with the formula:

$$R_o = \frac{1}{h_o} \tag{24}$$

Where h_o is the convection coefficient of the outside media (in the case calculated in this thesis the ocean)

The total thermal resistance through one cell is shown on Figure 21 and is expressed with the formula:

$$R_{total} = R_i + R_{cooper} + 2 * R_{ceramic} + R_{cell} + R_o \tag{25}$$

To be able to calculate the convection coefficient at each position the formula for the Nusselt number in natural convection is used:

$$Nusselt = C * (Gr * \mathrm{Pr})^n \tag{26}$$

Where C and n are the constants dependent on the geometry of the calculated item, Pr is the Prandtl number listed in heat transfer book tables [28] and Gr is the Grashof number and is expressed with the formula:

$$Gr = \frac{g * \beta(T_s - T_\infty) * L}{v^2} \tag{27}$$

Where g is gravitational acceleration, β is the volume expansion coefficient, T_s is the surface temperature of the outer plate seen on Figure 21and Figure 23, T_∞ is the ocean temperature, L is the height of the device calculated and v is the kinematic viscosity of the ocean water.

The Nusselt number equation (equation 26) can be rearranged. Rearranging the equation the convection coefficient can be determined and is expressed with the formula:

$$h_o = \frac{Nusselt}{k * L} \tag{28}$$

Where k is the thermal conductivity of the fluid (in this case water) at given temperature and L is the characteristic length of the calculated device.

The power output for one cell is then expressed with the formula:

$$Cell_{power} = \frac{\left[\frac{V}{2}\right]^2}{R_L} \tag{29}$$

Where V is the open circuit voltage and R_L is the load resistance.

3.4.1. Thermoelectric Efficiency

Efficiency for thermoelectricity can be calculated according to the first law of thermodynamics and can be expressed with the formula:

$$\eta_{th} = \frac{\dot{W}_{net}}{\dot{Q}_{in}} \tag{30}$$

But when the temperature is not constant in each area the thermal heat going through each cell will not be the same and therefore there will be different efficiency at each area.

3.5. Cost Analysis

In order to get an idea about the actual cost for each scenario an order of magnitude cost assumption was carried out. Included in the cost is the total cost of each component i.e. installation cost and all other cost needed to get a fully developed power plant.

The exploration cost for offshore geothermal is not fully know. The cost for exploration on land was considered to be $150/kW [29] that is 150 U.S dollars for each kW of installed electricity production. In most cases for offshore exploration a vessel will be needed [6]. When a vessel is used to explore more manpower is needed, leading to a higher cost. From that information the cost of offshore exploration was considered to be at least three times the cost on land. The cost used for exploration will therefore be $450/kW. The highest power output cycle calculated is then used to determine the exploration cost for all the cycles.

The drilling cost for offshore production wells is estimated to be at least twice the cost of drilling on land. That estimation was done considering the same as in estimating exploration cost, which is drilling from a vessel with more manpower need and therefore a higher cost. Cost for on land drilling was considered to be $750/kW [29]. That results in the cost for offshore drilling being $1500/kW. The highest power output cycle calculated is then used to determine the exploration cost for all the cycles.

Power plant cost for traditional power plants located on land is well documented. The cost for single a flash plant located on land was considered to be $1.656/kW [29].

Option A, power plant located on a platform has the same components as a traditional power plant located on land. It will be considered that a platform based plant will cost at least three times more than a traditional power plant. This assumption was made as the platform based power plant will cost the same as the traditional power plant but the installation and the platform cost will be much higher. The cost for option A will therefore be $4.968/kW.

Option B, power plant on land with a separator located at the ocean bed. For the separator reason the cost for a power plant located on land will be considered to be 50% higher than the cost of a traditional power plant on land. The cost for option B will therefore be $2.484/kW.

Option C, underwater power plant will be considered to cost four times more than a traditional power plant on land as the power plant needs to withstand a huge pressure (hydrostatic) from the seawater surrounding it as well as having a greater installation cost when working in such a difficult location. The cost for option C will therefore be $6.624/kW

Cost for a binary plant located on land is well documented. The cost for such a power plant is considered to be $2.615/kW [29].

Option D, binary power plant will be located on land and has a heat exchanger located at the ocean bed. For this reason the cost for the binary power plant will be estimated to be 50% higher than the cost of a traditional binary power plant. The cost for option D will therefore be $3.922 /kW

Operation and maintenance (O&M) cost is referred to as a percentage of the capital cost. The O&M cost is considered to be 4% of capital cost for a traditional single flash power plant located on land and 6% of the capital cost for a binary power plant located on land [29]. From this information, considerations for the four scenarios are estimated to be; 4% of the capital cost for a single flash power plant located on land (Option B), 5% of the capital cost for a single flash located on a platform (Option A), 10% of the capital cost for an underwater power plant (Option C) and 6% of the capital cost for a binary plant located on land (Option D). The 10% decision for option C was an estimation done according to the location of the plant, just reaching the plant with manpower will have more cost than for a land based power plant along with other basic power plant service. The 5% decision for option B is also made because of the location.

The pipe gathering system was approximated considering information from the engineering firm Mannvit [30]. The pipeline cost varies with the size; the larger the pipeline is the more it will cost. The pipeline size and length is different for each scenario and is shown in more details in section 4.6.1. The actual pipe lengths were estimations made regarding the power plant´s position.

The cost for thermoelectric power was considered with regard to the weight of steel and after literature search of thermoelectricity cost. The material needed for producing one square meter of thermoelectric device consist of a well-insulated steel box on five sides and one thermoelectric side where the heat flows through. The thermoelectric side consists of two copper plates, two ceramic plates and the thermoelectric cells. One of the copper plates is located in the device facing the geothermal fluid and the other copper plate is facing the ocean. The ceramic plates are located between the copper plate and the thermoelectric cells.

The cost for the steel is $7,5/kg [26] and for the cells, copper and ceramic plates it is estimated to be $1.500/$m^2$ [31]. The cost for the electrical device is assumed to be $1.500/$m^2$

[31]. The drilling and the exploration cost are assumed to be the same as the cost calculated in the drilling and exploration section for the binary cycle. As in previous costs installation cost along with all the necessary cost for the device to work is included in the total cost.

4. Results

4.1. Single Flash Cycle Calculation

There were three scenarios of single flash cycle calculated:

- Platform based power plant where the steam goes through a pipeline from the seabed to the platform (Option A)
- Land based power plant separating the two phase fluid at the seabed then directing the pure steam onto land via pipeline (Option B)
- Underwater power plant producing electricity and transporting it to land (Option C)

All the power cycle are calculated out from having one geothermal well drilled.

4.2. Properties for a Single Flash Power Plant

The properties needed to calculate the power output from a single flash power plant is the enthalpy, pressure and mass flow at each state. The pressure along with the corresponding mass flow from the regression curve on Figure 15 is optimized to maximize the power output of the cycle according to equation 30. The enthalpy used in this case is the average enthalpy from several production wells at the Reykjanes power plant and can be seen in appendix 1 and Table 1. Table 2 summarizes the optimal pressure and mass flow.

Table 2 Power plant´s optimal pressure and mass flow

Power Plants	Enthalpy [kJ/kg]	Optimal Pressure at Turbine Inlet [bar-a]	Optimal Mass Flow $\dot{m}_1$ [kg/s]	Optimal Steam Mass Flow $\dot{m}_3$ [kg/s]
Flash Plant Platform	1570	12,06	46,12	17,89
Flash Plant Underwater	1570	12,06	46,12	17,89
Flash Plant on Land	1570	12,06	45,72	17,2

The mass flow rate was calculated from a fitted simulated regression curve on Figure 15 as described in section 3.1.1. The formula for that is expressed like shown on Figure 15 and is:

$$\dot{m}_{geo\ fluid} = A * P_1^2 + B * P_1 + C \quad (31)$$

Where $\dot{m}_{geo\ fluid}$ is the mass flow of the geothermal fluid, P_1 is the pressure at state 1 and A B and C are constants calculated so the regression curve fits the given input data. This regression curve formula was then used for calculating the optimal pressure and mass flow in all the scenarios.

4.2.1. Power Plant on a Platform

This power plant option is based on the idea of having the power plant on a platform. A pipeline is needed from the seabed to the platform to direct the fluid from the reservoir to the separator. It is estimated that the pipeline is like an extension of the reservoir so there is no two phase flow in the pipeline concerned. The approximated depth between the platform and ocean bed was set to be between 150-300 meters. The calculations were done from the higher value of 300 meters. That depth is shown on Figure 1. All calculations were done in EES and can be found in appendix 3. Figure 24 is a conceptual drawing showing the components with regard to each other.

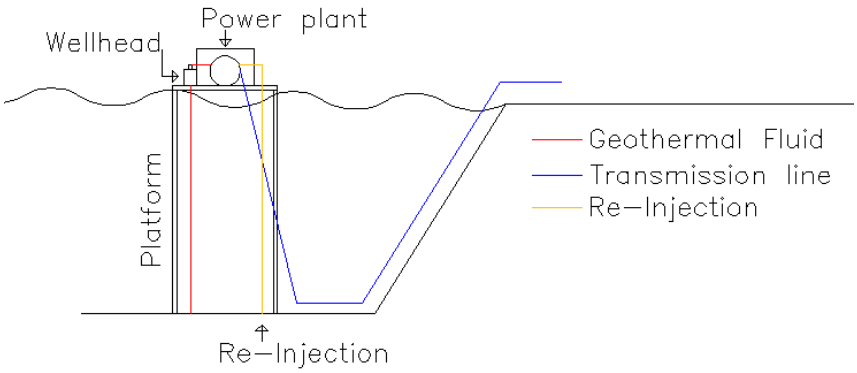

Figure 24 Platform based power plant

4.2.1.1. Pressure Loss and Pipe Sizing Calculations

The pressure loss was calculated with the EES software and with the formulas shown in section 3.2.11. Table 3 shows the actual velocity, commercial pipe diameter, commercial pipe thickness and the pressure loss for each pipeline marked with each state number. The commercial pipe diameter was chosen from the calculated diameter [32]. The pressure loss in Table 3 was multiplied with 2 to count for the fittings needed with the pipeline design and the pressure loss is not high due to the actual pipe length. The pipe length used for calculations was estimated and should be readjusted to the designed pipe length.

Table 3 Pressure loss and pipe sizes

State Number	Velocity [m/s]	Actual Velocity [m/s]	Calculated Diameter [mm]	Commercial Diameter [mm]	Calculated Thickness [mm]	Commercial Thickness [mm]	Pressure Design [bar]	Pipe Length [m]	Pressure loss [bar]
1	2,5	2,3	1222	1321	18,9	20	-	300	0,00190
2	30	29,3	351,1	355,6	7,3	8	25	10	0,02371
3	30	24,4	351,3	406	7,9	8	25	10	0,01157
4	30	30,7	3037	3105	40,3	50	25	5	0,00001
5	2,5	2,1	95,94	114,3	4,4	5	25	10	0,06903
6	2,5	0,1	3,221	60	3,7	4	25	10	0,00000
7	2,5	2,5	128	139	4,7	5	25	10	0,06390
8	2,5	2,4	453,7	483	8,8	11	25	10	0,01520
9	2,5	2,4	453	483	8,8	11	25	10	0,01516

4.2.1.2. Diagram Showing the Condition for Single Flash on Platform

Figure 25 is a diagram showing the condition of each state in the process. The diagram shows all the components as well as pressure, enthalpy, temperature, mass flow and the power output for each state in the single flash power cycle. Calculated results for each state are shown in appendix 3.

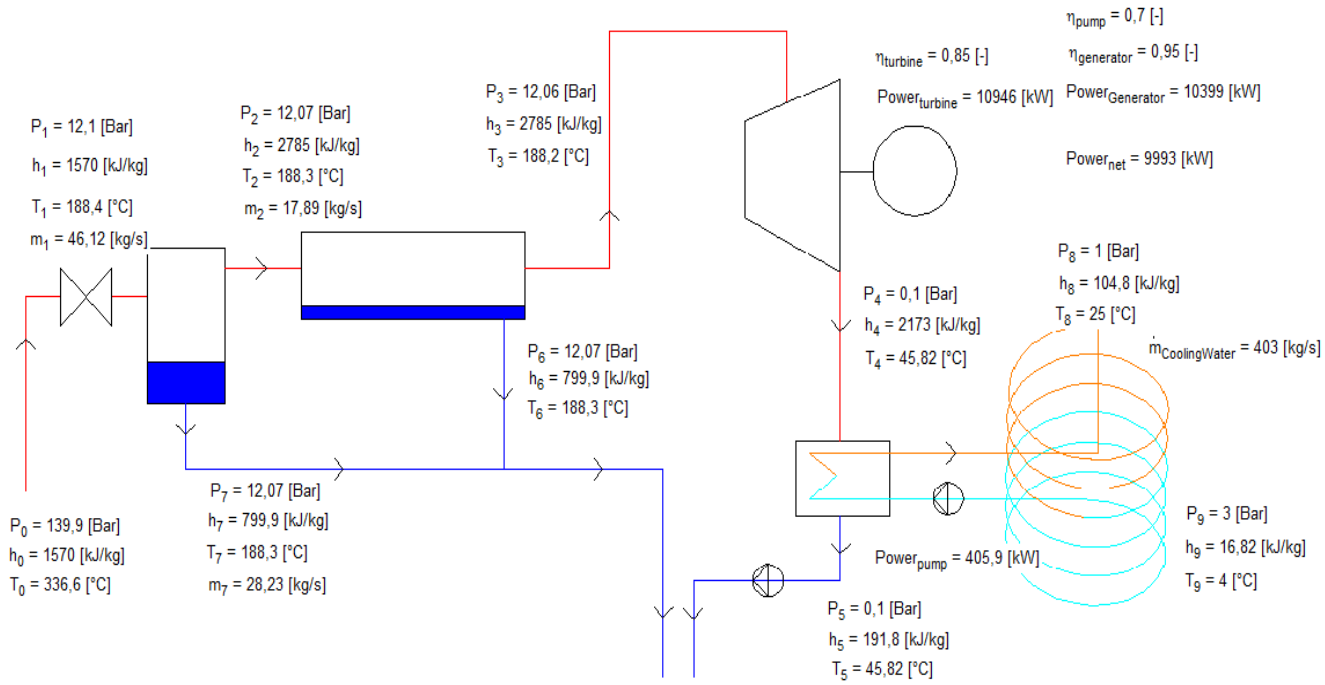

Figure 25 Diagram drawing for single flash on a platform with components placed in their position

4.2.1.3. Power Output for Single Flash on a Platform

The formulas used for the calculation are shown both in section 3 and in the EES code shown in appendix 3. The optimal pressure and mass flow were calculated to maximize the turbine power output. The optimization is shown on Figure 26.

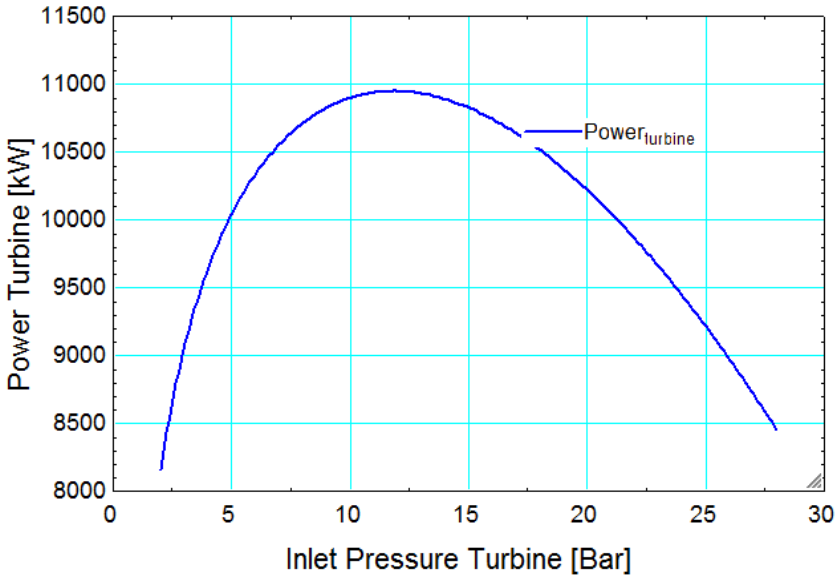

Figure 26 Plot power - pressure for single flash on platform

The turbine power output is then calculated with regard to optimal pressure being 10.946 kW_e. The generator has the efficiency 0,95 [25] and the cooling water pump needs 406 kW_e to be able to provide the necessary flow into the condenser. The net power output for the single flash is then calculated to be 9.993 kW_e.

4.2.2. Land Based Power Plant

This power plant option is based on the idea of having the power station located on land. To be able to situate the power plant on land a separator shall be located at the seabed as a two phase flow coming from the reservoir cannot flow upwards. If the two phase flow is to flow upwards an unstable flow pattern could occur like slug flow [21]. Slug flow can cause excessive vibration in the pipes [21]. The pipeline from the separator to the power plant is the main difference in calculations between the platform based power plant described in section 4.1 and the land based power plant described in this section. As can be seen in section 3 thermal losses are neglected and therefore it is estimated that the quality in the pipe line between the separator and the power plant is 100% steam. All calculations were done in EES and can be found in appendix 3. Figure 27 is a conceptual drawing of the components with regard to each other.

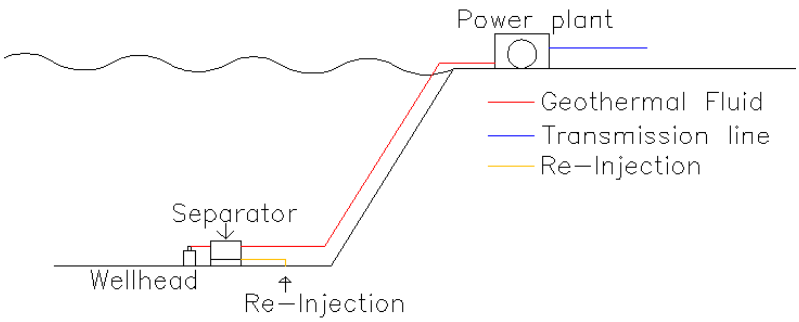

Figure 27 Land based power plant

The calculated pressure loss in land based power plant is the same as in platform based power plant and is shown in Table 3, except for the pipeline between the separator and the demister. The demister is located inside the power plant. The pressure loss for the pipeline between the separator and the demister goes from 0,023 bar pressure loss for platform based power plant up to 2,2 bar for land based power plant.

The turbine power output was calculated to be 10.523 kW_e. The cooling water pump needs 390,3 kW_e to be able to provide the necessary flow into the condenser. The net power output for the single flash power plant based on land was therefore calculated to be 9.607 kW_e.

4.2.3. Underwater Power Plant

This power plant option is based on the idea of having all of the components completely underwater. A transmission line is needed to transport the electricity to land. Calculations regarding the power output are almost the same as for platform based power plant except for the pump work for the cooling. The total head calculated is 0 meters when using underwater power plant compared to 50 meters in head for platform based power plant. The biggest difference between the power plants is the actual cost. The cost will be analyzed in section 4.5. All calculations are done in EES and can be found in appendix 3. Figure 28 is a conceptual drawing showing the components with regard to each other.

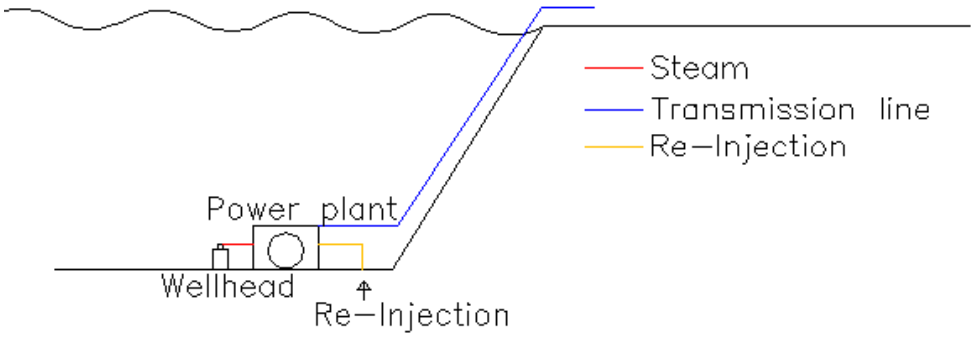

Figure 28 Underwater based power plant

The turbine power output was then calculated with regard to optimal pressure being 10.946 kW_e. The generator has the efficiency 0,95 [25] and the cooling water pump needs 129,2 kW_e to be able to provide the necessary flow into the condenser. The net power output for the underwater single flash plant was then calculated to be 10.269 kW_e.

4.3. Binary Cycle Power Plant

This power plant option is based on the idea of having a binary cycle power plant located on land. There are two options available for utilizing the energy of the geothermal fluid coming from the well head. A) Transporting the geothermal fluid to land in liquid form without flashing as a two phase flow cannot flow upstream. Doing that the pipeline would be at reservoir pressure and reservoir temperature. B) To have a heat exchanger located at the seabed transferring the working fluid from land based plant to the heat exchanger located on the seabed. Option B was chosen for the calculations performed in this research as the reservoir pressure was considered to be too high for the pipeline and theoretically it would be impossible to keep the pipeline without thermal and pressure loss all the way to land, such losses could cause the liquid to boil and transform it into a two phase flow. The exchanger at the seabed will heat up the working fluid to the turbine inlet state. The pipeline gathering system for the binary power plant is twice the length of the pipeline for the single flash plant because the pipeline goes both ways into the exchanger. As can be seen in section 3 thermal losses as well as changes in kinetic and potential energy are neglected and therefore it is estimated that the working fluid in the pipeline coming from the heat exchanger to the power plant will be superheated steam. All calculations were done in EES and can be found in appendix 4. Figure 29 is a conceptual drawing showing what it could look like.

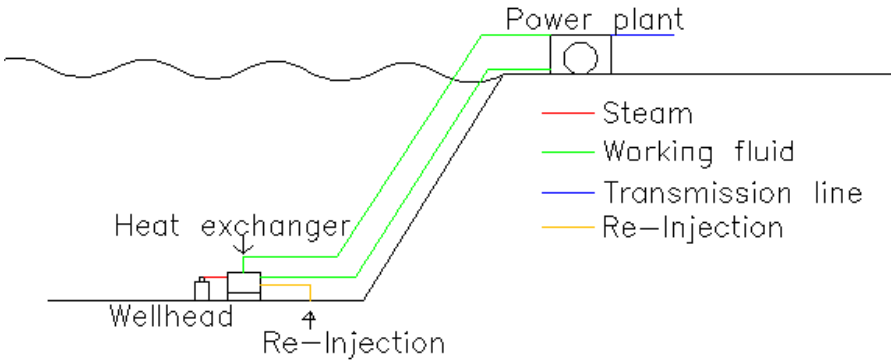

Figure 29 Binary power plant based on land

4.3.1. Properties for a Binary Power Plant

The properties used to calculate the binary cycle power plant are the enthalpy of the geothermal fluid, optimal geothermal pressure and the optimal mass flow for the geothermal fluid. The enthalpy of the geothermal fluid is the calculated average enthalpy from Table 1, or 1.570 kJ/kg. The pressure and mass flow of the geothermal fluid were optimized to give the maximal power output for the binary cycle. In this case the optimal pressure was calculated to be 19,14 bar and the total mass flow was calculated with the regression curve formula to be 43,87 kg/s.

4.3.2. Binary Fluid

A calculation regarding the best fitting working fluid was done in EES. The selected binary fluid used is methanol, it was chosen from calculations of several different fluids. Methanol gives the highest net power output and has a small specific volume compared to other binary fluids. There is one disadvantage though and that is the high 45 bar pressure inside the binary cycle as shown on Figure 31 and in Table 4. A comparison was done between several fluids that could be used and those fluids are listed in Table 4.

Table 4 Comparison of working fluid

Working Fluid	Power Turbine [kW]	Net Power [kW]	Pressure Steam [Bar-a]	Max Pressure Working Fluid State 1[Bar-a]	Pipe Size at State 1 [m]
Acetone	16.467	13.860	15,8	27,3	0,240
Benzene	15.855	13.754	16,3	13,9	0,244
Cyclohexane	14.852	12.769	15,6	12,7	0,298
Ethanol	15.872	13.438	16,3	29,7	0,194
Methanol	**16.449**	**14.086**	**19,1**	**45,4**	**0,174**
Isopropanol	15.585	13.432	15,7	23,7	0,209
Isopentane	14.879	11.414	11,2	30,3	0,310
m-Xylene	11.752	10.054	17,4	4,4	0,245
R113	15.651	12.696	15,1	25,2	0,293
R123	15.611	11.997	10,4	33,0	0,305

4.3.3. Power Output for Binary Cycle

The calculations for the binary were done in EES. The calculations for this type are the same as when calculating other binary plants on land, except for the pipelines coming to the heat exchanger from land are longer than normal as the heat exchanger is located at the ocean bed. The power output is maximized according to the optimal pressure and the optimal flow rate of the geothermal fluid, see Figure 30.

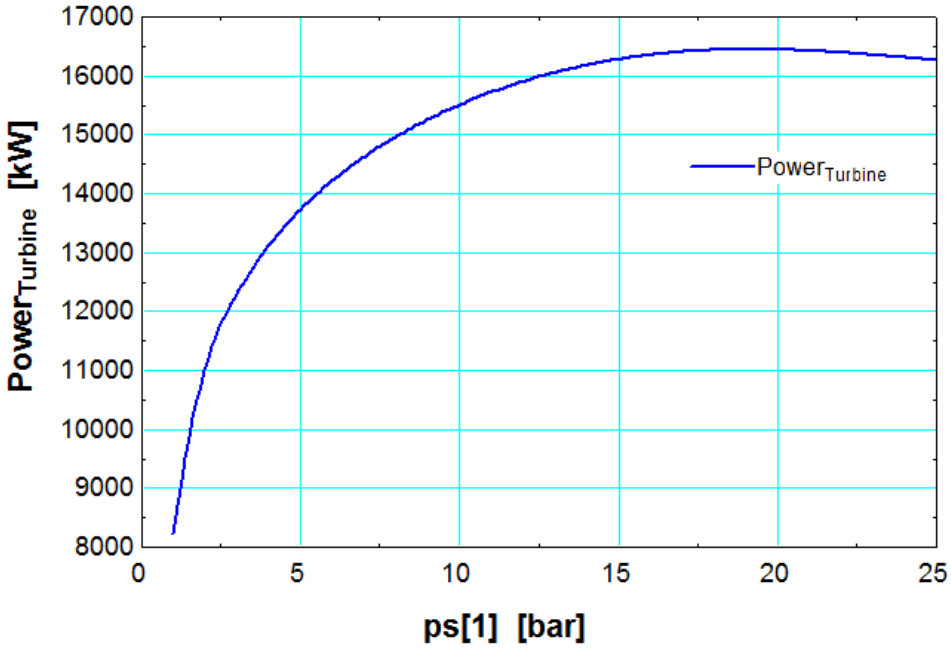

Figure 30 Plot power – pressure of geothermal liquid in binary cycle

The calculated turbine power output was 16.449 kW_e. The generator has the efficiency 0,95 [25] which leads the power output to go down to 15.626 kW_e. The pumps has the efficiency of 0,65 [25] and the power needed for the feed pump is 412,5 kW_e and for the cooling water pump 1.127 kW_e. After summarizing those numbers the net power output will become 14.086 kW_e.

4.3.4. Diagram Showing Condition for the Binary Cycle

Figure 31 is a diagram showing the condition at each state in the process. The diagram shows all the components as well as pressure, enthalpy, temperature, mass flow, heat flow and the power output. Calculated results for each state are shown in appendix 4.

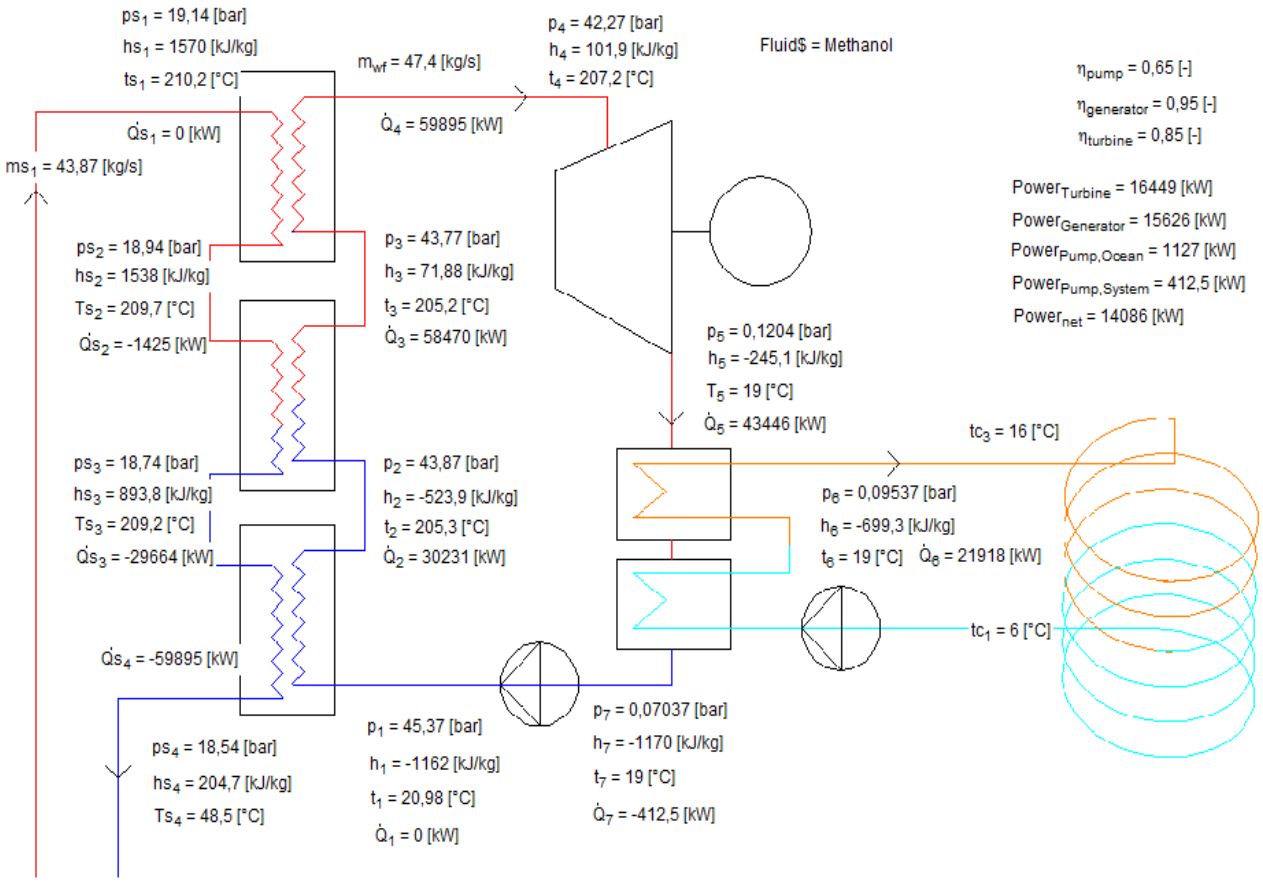

Figure 31 Process diagram of a binary cycle showing the conditions for each state

4.3.5. Heat Exchanger Calculation

The heat exchange in the heat exchanger is shown on Figure 32 and the corresponding states can be seen on Figure 31. States 4s and 1 to states 3s and 2 is where the working fluid will enter the preheat exchanger for pre heating the working fluid to saturation liquid phase. States 3s and 2 to state 2s and 3 is where the working fluid evaporates from saturated liquid to saturated vapor phase. State 2s and 3 to state 1s and 4 is where the working fluid is super-heated to superheated steam before entering the turbine. The pinch for the heat exchanger is set to be 3°C [25] and the superheated steam goes up by 2°C [25]. The heat can be seen on the x axis on Figure 32 where it is attached to each state.

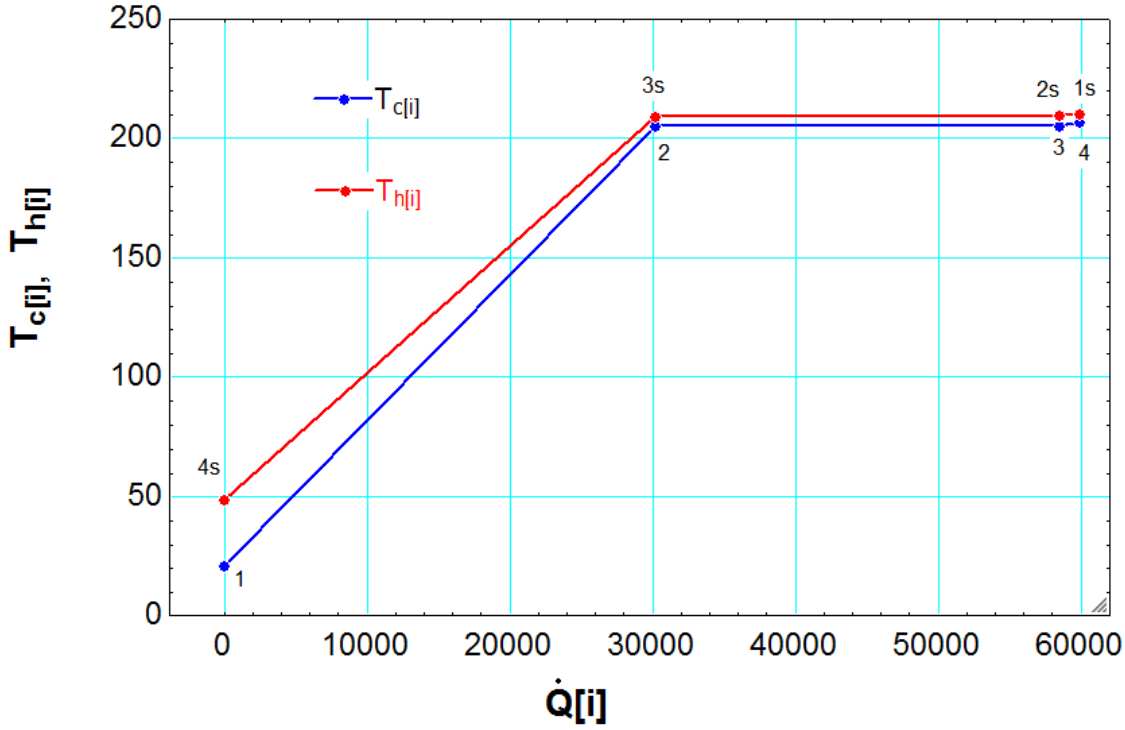

Figure 32 The heat exchange process showing how the heat is transferred from the geo-fluid to the working fluid

On Figure 32 the red line represents temperature of the geothermal fluid (T_h) and the blue line represents the temperature of the working fluid (T_c) and Q is the thermal heat transferred between the two fluids.

4.3.6. Condenser

The condenser is shown on Figure 33 and the corresponding states can be seen on Figure 31. The steam coming from the turbine needs to change phases from steam to liquid form for re-pumping the working fluid into the heat exchanger. The temperature of the working fluid does not change through the condenser. The main change is in the enthalpy of the working fluid. At

state 1c which is the condenser inlet the temperature is set to be 6°C as that is the oceans average temperature in Reykjanes [8].

As shown on Figure 33, heat is being rejected from the working fluid to the ocean fluid and the ocean fluid is condensing the working fluid to a liquid phase before the working fluid is pumped back into the heat exchanger. The pinch in this case was set to be 3°C [25]. The lower the pinch is the bigger the surface area of the condenser needs to be and more work is needed for the condensing pump. To estimate the actual pinch and pump size for each case, profitability calculations are needed to calculate the most profitable economic model for given situation.

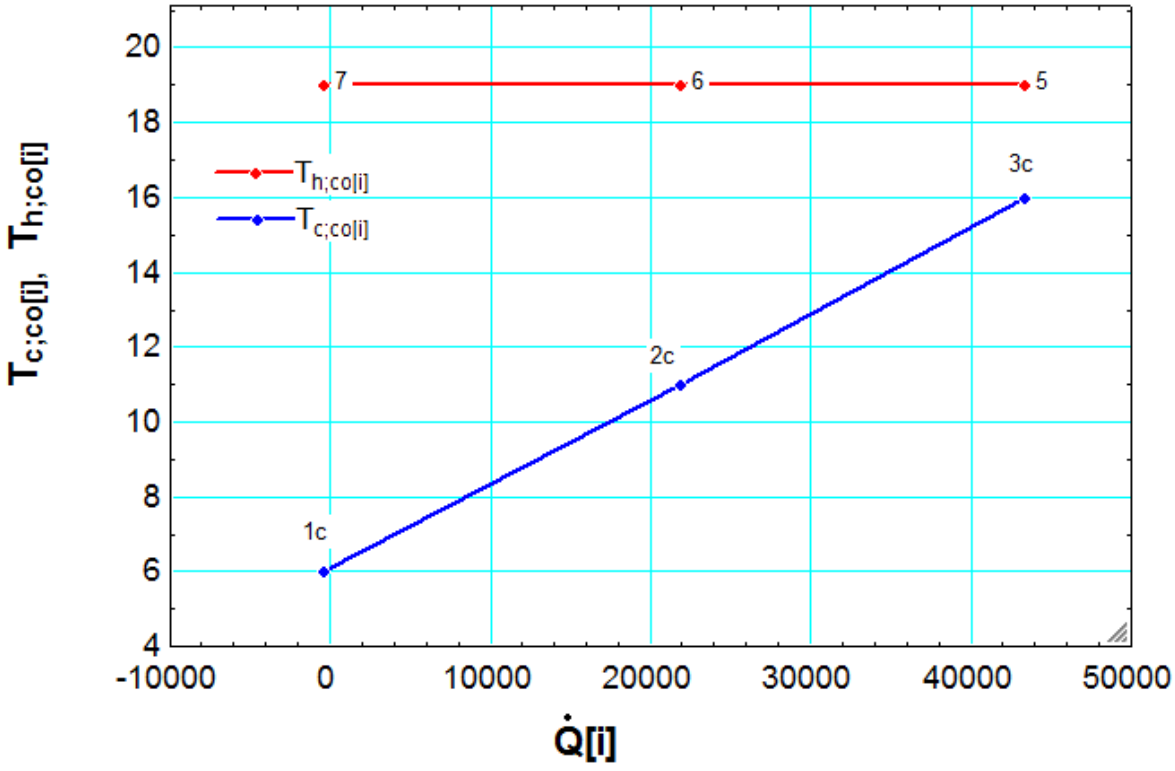

Figure 33 The condenser showing how the heat is rejected from the condensing working fluid to the cooling fluid

On Figure 33 the red line represents the temperature of the working fluid ($T_{h:co}$) and the blue line represents the temperature of the ocean fluid ($T_{c:co}$) and Q is the thermal heat transferred between the two fluids.

4.3.7. Pressure Loss and Pipe Sizing in Binary Cycle

A precise pressure loss calculation was not done for the binary cycle. Estimation for each state was therefore made for the pressure loss and those numbers can be seen in appendix 4 and in Table 5. The pipe sizing was calculated to the required diameter for a given velocity. Commercial pipe sizes were not found for the binary cycle.

Table 5 Pressure loss estimation and pipe sizing

State Number	Velocity [m/s]	Actual Calculated Diameter [mm]	Pressure Design [bar]	Pipe Length [m]	Estimated Pressure loss [bar]
1	2,5	174,3	46	1000	1,5
2	2,5	212,6	46	10	0,1
3	30	187,6	46	10	0,1
4	30	196,8	46	1000	1,5
5	30	3105	25	10	0,025
6	2,5	8658	25	10	0,025
7	2,5	2203	25	10	0,1

4.4. Thermoelectric Power Calculations

To calculate the actual power output for a given situation, information regarding some parameters are needed. Those parameters are the depth down to the seabed where the thermoelectricity equipment is located and is set to be 150 meters, the inlet temperature of the geothermal fluid which is considered to be 180 °C and the ocean temperature considered to be 5 °C down at 150 meters.

The convection heat transfer coefficient for the geothermal fluid is estimated to be 5000 W/m^2K and the convection heat transfer coefficient for the cold ocean side is variable with regard to temperature and length shown on Figure 21 and Figure 23. Therefore calculations with different delta ΔT are performed; those calculations were done with Matlab and are in appendix 5. The data used for calculations where all collected from the same thesis [27] and heat transfer book [28]. In the thesis [27] an experiment was done in a laboratory in Cardiff University. This experiment was done to map how much electricity one cell could produce. The results were plotted and a regression line fitted in graph along with the calculated ΔT. The ΔT is marked with colored lines on Figure 34.

The cell used for calculations is considered to be 40 x 40 square millimeter with a thickness of 3,5 millimeter. This cell is the same cell as used in the experiment and for the regression line described before.

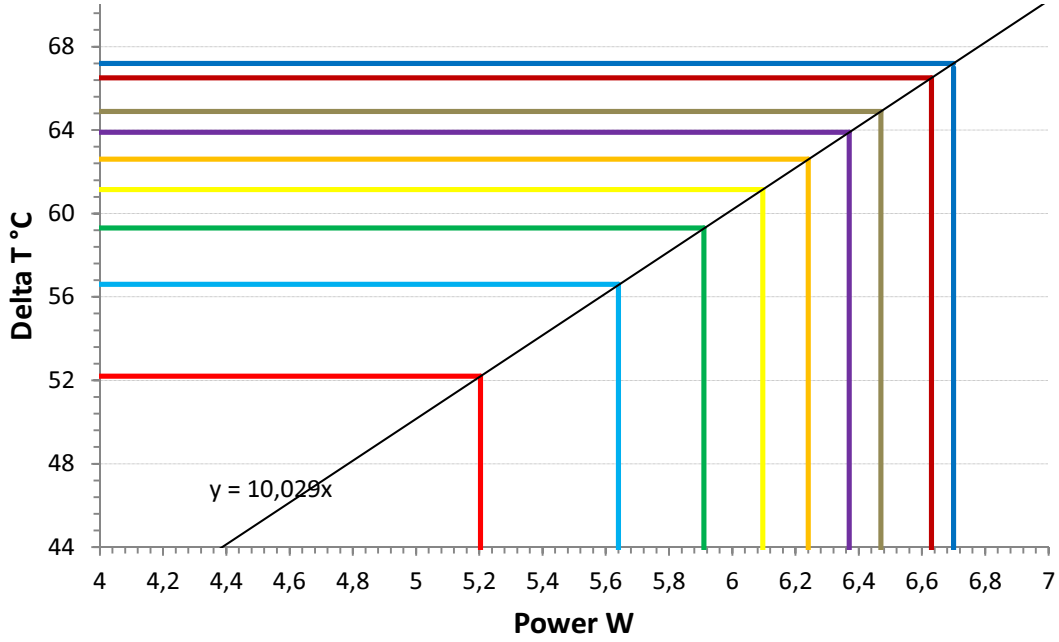

Figure 34 Regression graph showing power for one cell for given ΔT

When the regression line was fitted to its place and calculations done for the ΔT (Matlab code in appendix 5) over one cell, calculations for 1 m^2 of thermoelectricity device could be done. The area of 1 m^2 was divided into 10 equal areas which all have different ΔT. The geothermal fluid going in the device is two phase flow at the temperature of 180°C. The mass flow is not calculated as the device is consider to have enough flow to have the device at constant temperature of 180°C. It was calculated that for every area with the geometry of 0,1 meter times 1 meter, 59 cells could be fitted in that area see Figure 23. Calculations with regard to that are shown in Table 6.

Table 6 Power calculations for thermoelectricity

Area	ΔT [^{o}C]	Power for One Cell in [W]	Number of Cells [10cm x100cm]	Power per Area [W]
1	67,2	6,70	59	395,3
2	66,5	6,63	59	391,2
3	65,8	6,56	59	387,1
4	64,9	6,47	59	381,8
5	63,9	6,37	59	375,9
6	62,15	6,20	59	365,6
7	61,15	6,10	59	359,7
8	59,3	5,91	59	348,9
9	56,6	5,64	59	333,0
10	52,2	5,20	59	307,1
Total Power Output [W]				3645,7

From calculations in the power output for 1m^2 of thermoelectricity equipment as shown on Figure 23 it is approximately 3,6 kW. If thermoelectricity should be equal to the highest power output calculated before, which is the binary cycle producing 14.086 kW, the size of the thermoelectricity has to be 3.863 square meters. That could e.g. be a plate that is 100 meter wide and 1 meter high. Approximately 39 plates would be needed to for fill the same power output for the binary plant.

4.4.1. Thermoelectric Carnot Efficiency

The thermoelectric Carnot efficiency was calculated in Matlab and is expressed after the first law of thermodynamics shown in equation 30 and is calculated to be 15,2 at the first area and 11,8 at the last area shown on Figure 23. The average Carnot efficiency for all the areas shown on Figure 23 is then 12,9.

4.5. Power Output Comparison

After analyzing each utilization option in section 4 a comparison table between their power output and cost was made. That way it can be seen which power option fits Reykjanes area best for offshore utilization.

Table 7 Comparison of power options

	Unit	Single Flash			Binary Cycle	Thermoelectricity for one square meter
		Platform	Land Based	Under Water		
Power Turbine	kW	10.946	10.523	10.946	16.449	
Power Pump Ocean	kW	406	390,3	129,2	1127	
Power Feed Pump	kW				412,5	
Power Generator	kW	10.399	9.997	10.399	15.626	
Power Net	kW	9.993	9.607	10.269	14.086	3,645
Exergy Efficiency	%	49	44	47	65	

Table 7 shows the power output for each power station. The binary cycle gives the highest net power output. All the options were calculated to maximize the power output using the optimal pressure and optimal mass flow. The exergy efficiency seams a bid high but the reason for this is the high utilization ratio of the geothermal fluid enthalpy.

4.6. Cost Analysis

Order of magnitude cost assumptions was carried out for all the scenarios in section 4. The cost for each component was calculated as shown in tables in the following sections.

4.6.1. Pipeline Cost

The cost for the pipeline gathering system is calculated form information gathered from the engineering firm Mannvit [30]. Table 8 shows the cost for different pipe size after the calculated diameter for each case in section 4.

Table 8 Cost for pipe line gathering system

Pipe Gathering System for Each Case	Pipe Lines in Meters	Pipe Diameter [m]	Pipe Prize per Meter [$]	Total Prize Pipe [$]
Flash Plant Platform	300	1.320	920	276.000
Flash Plant Underwater	20	1.320	920	18.400
Flash Plant on Land	1.000	1.180	710	710.000
Binary Plant	2.000	200	520	1.040.000
Thermoelectric	200	200	520	104.000

4.6.2. Power Plant Cost

The exploration and drilling cost is calculated as a fixed cost per kilowatt in the binary station as it gives the highest power output. The same exploration and drilling cost is then used for all the scenarios. The capital cost and O&M cost is analyzed in section 3.5. Calculation results are shown in Table 9,Table 10,Table 11 and Table 12.

Table 9 Cost for single flash power plant based on a platform

Single Flash Plant Platform	Size in [kW]	Cost/kW [$]	Capital Cost [$]	Offshore Factor	Total Cost [$]
Exploration			2.467.350	3	7.402.050
Drilling			12.336.750	2	24.673.500
Flash Plant Platform	10.946	1.656	18.126.576	3	54.379.728
O&M 5% of Cap Cost			906.329		906.329
Pipe Line for Gathering System			276.000	3	828.000
Total Cost					**88.189.607**
Total Cost per kW					**8.057**

Table 10 Cost for land based power plant with a separator located at the ocean bed

Single Flash Plant on Land	Size in [kW]	Cost/kW [$]	Capital Cost [$]	Offshore Factor	Total Cost [$]
Exploration			2.467.350	3	7.402.050
Drilling			12.336.750	2	24.673.500
Flash Plant on Land	10.523	1.656	17.426.088	1,5	26.139.132
O&M 4% of Cap Cost			697.044		697.044
Pipe Line for Gathering System			710.000	3	2.130.000
Total Cost					**61.041.726**
Total Cost per kW					**5.801**

Table 11 Cost for single flash power plant underwater

Single Flash Plant Underwater	Size in [kW]	Cost/kW [$]	Capital Cost [$]	Offshore Factor	Total Cost [$]
Exploration			2.467.350	3	7.402.050
Drilling			12.336.750	2	24.673.500
Flash Plant Under Water	10.946	1.656	18.126.576	4	72.506.304
O&M 10% of Cap Cost			1.812.658		1.812.658
Pipe Line for Gathering System			18.400	3	55.200
Total Cost					**106.449.712**
Total Cost per kW					**9.725**

Table 12 Cost for the binary cycle plant based on land with heat exchanger located on the ocean bed

Binary Plant	Size in [kW]	Cost/kW [$]	Capital Cost [$]	Offshore Factor	Total Cost [$]
Exploration	16.449	150	2.467.350	3	7.402.050
Drilling	16.449	750	12.336.750	2	24.673.500
Binary Plant	16.449	2.615	43.014.135	1,5	64.521.203
O&M 6% of Cap Cost			2.580.848		2.580.848
Pipe Line for Gathering System			1.040.000	3	3.120.000
Total Cost					**102.297.601**
Total Cost per kW					**6.219**

4.6.3. Thermoelectricity Cost

The cost for the drilling and exploration are considered to be the same as the cost calculated in the binary section. The O&M cost is calculated to be 10 times the device cost and is analyzed in section 3.5. Calculation results are shown in Table 13 and Table 14.

Table 13 Cost for one square meter of thermoelectricity device shown in Figure 23

Thermoelectricity Device for $1m^2$ (shown on Figure 23)	Length [m]	Width [m]	Height [m]	Density steel [kg/m3]	Total steel [kg]	Cost [$]
Steel backside (I side)	1	1	0,01	7.870	78,7	
Steel sides (4 sides)	1	0,2	0,01	7.870	62,96	
Extra steel inside (7 * steel for sides)				7.870	440,72	
Total weight steel					582,38	
Cost for 1 Kg steel = $7,5/kg						4.368
Cost for Copper plates and cells = $1500/$1m^2$						1.500
Cost for electrical device = $1500/$1m^2$						1.500
Total cost for $1m^2$ device						**7.368**

The calculations in Table 14 are done for 3863 m^2 of thermoelectric device shown on Figure 23. More detailed analysis is needed to determine how much geothermal fluid will be needed to fill the requirement of producing 3,6 kW of power in one square meter of thermoelectric device and therefore it is estimated that three wells would be enough to for fill the need.

Table 14 Total cost for $1m^2$ of thermoelectric device shown on Figure 23

Thermoelectricity Power	Size in [kW]	Cost/kW [$]	Capital Cost [$]	Offshore Factor	Total Cost [$]
Exploration		150	2.467.350	3	7.402.050
Drilling (3 wells considered)		750	37.010.250	2	74.020.500
Pipeline for Gathering System			104.000	3	312.000
Device for 3863 m^2	14.086,0				28.462.005
O&M 10 times the device cost					73.679
Total Cost					**110.270.233**
Total Cost per kW					**7.828**

5. Discussion

Data shows that the area around Reykjanes peninsula has seismic activity and could possibly be a feasible choice for offshore geothermal utilization. In this thesis several power processes and configurations were analyzed and calculations made for the net power output and economical cost for each option. The results show that regarding the net power output only the binary power plant would be the most feasible option. On the other hand with respect to $/kW ratio, the single flash power plant located on land turns out to be the most realistic choice. Although the single flash located on land has the best $/kW ratio it could turn out to be too expensive. Factors like increased distances from land based plant to the source or wellhead will automatically change the cost calculations for the land based power plants, as land based power plant cost increases with longer pipelines.

Thermoelectricity could be a favorable future power option and calculations show that one square meter of thermoelectricity device shown on Figure 23 could produce approximately 3,6 kW. More analyses are needed to estimate how many square meters of thermoelectric device one geothermal well can provide. After such analyses the real total cost per kW can be calculated. Further cost calculations are needed to evaluate more realistic economic feasibility for thermoelectric power.

6. Conclusion

It is concluded that offshore power plants are technically possible although many questions are still unanswered when it comes to detailed design of offshore power plant. Economically it is not feasible at least not when there is still geothermal energy to be utilized on land. The energy price has a big effect on the future development for offshore projects i.e. if the energy prices increase dramatically then development of projects like the offshore geothermal might be faster. The thermoelectric power option is not comparable with other power cycles as more detailed cost analyses are needed.

7. Future Work

In this thesis, a number of configurations and energy processes for offshore power utilization were analyzed and compared, regarding power output and economical aspects. There are still many questions unanswered on offshore power utilization and those questions need further study. Some of the further studies necessary could be;

- A detailed offshore power plant design taking into account all the components needed in a fully designed power plant. Those components would include transmission lines, separator, demister, turbine, condenser and other important components needed for detailed design.

- Making detailed environmental assessment for the process of offshore geothermal utilization. That could be for the power plant location and the offshore drilling part. The offshore drilling could cause some disturbance to the wild sea life and for that reason there is need for an environmental assessment.

- To conduct a more detailed cost analysis for all the configurations analyzed in the thesis, the cost analyzed here is an order of magnitude assumption and for that reason it may be considered as a rough estimation.

- A detailed scaling analysis for the pipeline gathering system, as the wellhead pressure for each scenario was selected with regard to the maximal power output instead of selecting it with regard to scaling effect. In real situations problems could occur with scaling at a given pressure. In those cases the pressure needs to be adjusted to the pressure where there is less effect of scaling in the pipeline gathering system. Then the power output might be even lower than the actual power output calculated before.

- The amount of non-condensable gases coming with the geothermal fluid will need to be accounted for as it lowers the mass flow of steam entering the turbine and increases the parasitic load.

8. References

[1] G. Þórólfsson, “Information about the Reykjanes area.”

[2] Á. Höskuldsson, R. Hey, E. Kjartansson, and G. B. Guðmundsson, “The Reykjanes Ridge between 63°10′N and Iceland,” *Journal of Geodynamics*, vol. 43, no. 1, pp. 73–86, Jan. 2007.

[3] “REM - Renewable Energy Mediterranean - home.” [Online]. Available: http://www.remenergy.it/home.php?Lang=en.

[4] “Marsili Project.” [Online]. Available: http://www.eurobuilding.it/marsiliproject/index.php?option=com_content&view=article&id=54&Itemid=61.

[5] G. Hiriart, R. M. Prol-Ledesma, S. Alcocer, and G. Espíndola, “Submarine geothermics: Hydrothermal vents and electricity generation,” in *Proceedings World Geothermal Congress*, 2010.

[6] D. Atkins, “Exploration Techniques for Locating Offshore Geothermal Resources near Iceland,” Reykjavík University REYST, Reykjavík, 2013.

[7] J. Benjamínsson, “Jarðhiti í sjó og flæðarmáli við Ísland,” Marine Research Insitute, 1988.

[8] Á. Höskuldsson and E. Kjartansson, “Gosbergshryggir á hafsbotni og sambærilegar myndanir á landi, Dyngjufjöll Ytri.,” Jarðfræðafélag Íslands, 2005.

[9] U. Stefánsson and J. Ólafsson, “Nutrients and fertility of Icelandic waters,” University of Iceland and Marine Research Institute, Mar. 1991.

[10] V. Harðardóttir, “Metal-rich Scales in the Reykjanes Geothermal System, SW Iceland: Sulfide Minerals in a Seawater-dominated Hydrothermal Environment.” [Online]. Available: http://www.ruor.uottawa.ca/en/handle/10393/19925?show=full.

[11] J. Pettersen, “LysarkPettersen2011B.pdf.”

[12] “Transocean :: Discoverer Clear Leader.” [Online]. Available: http://www.deepwater.com/fw/main/Discoverer-Clear-Leader-697.html.

[13] S. Þórhallson, “Offshore drilling technology,” July 20.

[14] P. Skalle, *Pressure Control During Oil Well Drilling*. BookBoon.

[15] S. Þórhallson, “Geothermal Wells and Drilling Technology,” Reykjavik University.

[16] “NORSOK Standard D-010; Well integrity in drilling and well operations.” Standards Norway, 2004.

[17] K. Sæmundsson, “Jarðhitasvæðið á Reykjanesi | Íslenskar orkurannsóknir,” *isor.is*. [Online]. Available: http://www.isor.is/efni/jardhitasvaedid-reykjanesi. [Accessed: 17-Oct-2012].

[18] “Orkuvefsjá.” [Online]. Available: http://www.orkuvefsja.is/vefsja/orkuvefsja.html.

[19] P. Jónsson, “Production curves,” Aug-2012.

[20] P. Jónsson and H. Björnsson, “Svartsengi - Reykjanes Hita- og þrýstingsmælingar 2010,” Ísor Iceland Geosurvey, May 2011.

[21] R. DiPippo, *Geothermal Power Plants: Principles, Applications, Case Studies and Environmental Impact*, Second Edition. North Dartmouth, Massachusetts: .

[22] Y. A. Cengel and M. A. Boles, *Thermodynamics An Engineering Approach*, Seventh Edition in SI Units. McGraw-Hill.

[23] J. W. Lund, “Direct heat utilization of geothermal resources,” *Oregon Institute of Technology*, 2000.

[24] Þ. Jóhannesson, “Power Plant Design.”

[25] P. Valdimarsson, “Power Plant Design.”

[26] W. Harvey, “Gathering System and Pipe Sizing,” Rykjavik University, Iceland.

[27] B. Þ. Hafsteinsson, “Vinnslunýtni varmarafmagns,” Meistaraverkefni, Háskóli Íslands, 2002.

[28] F. P. Incropera, D. P. Dewitt, T. L. Bergman, and A. S. Lavine, *Introduction to Heat Transfer*, Fifth Edition. .

[29] C. N. Hance, “Factors Affecting Cost of Geothermal Power Development - August 2005.pdf,” Geothermal Energy Association, Aug. 2005.

[30] K. Ingason, “Cost for Pipe Lines.”

[31] Á. Geirsson, “Information about the cost for thermoelectricity; Former owner of Varmaraf (thermoelectric company).”

[32] “Standard Pipe Sizes EN10220_GB.pdf.” [Online]. Available: http://www.stahlrohr.eu/pdf/EN10220_GB.pdf.